Using Polymer Electrolyte Membrane Fuel Cells in a Hybrid
Surface Ship Propulsion Plant to Increase Fuel Efficiency
by
Douglas M. Kroll
B.S., Electrical Engineering, Virginia Tech, 2001

Submitted to the Department of Mechanical Engineering and Engineering Systems
Division in Partial Fulfillment of the Requirements for the Degrees of
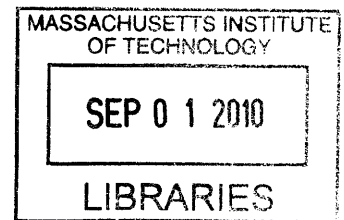
Naval Engineer
and
Master of Science in Engineering and Management

at the
Massachusetts Institute of Technology
June 2010

© 2010 Douglas M. Kroll. All rights reserved.

The author hereby grants to MIT permission to reproduce and to distribute publicly
paper and electronic copies of this thesis document in whole or in part in any medium now known or
hereafter created.

Signature of Author..   ....
Department of Mechanical Engineering and
Systems Design and Management Program
\ / /May 7, 2010

Certified by...
Mark S. Welsh
Professor of the Practice, Naval Construction and Engineering
Thesis Supervisor

Accepted by...
Pat Hale
Director, System Design and Management Fellows Program
Engineering Systems Division

Accepted by...
David Hardt
Chairman, Department Committee on Graduate Studies
Department of Mechanical Engineering

	Form Approved OMB No. 0704-0188

Report Documentation Page

1. REPORT DATE **JUN 2010**	2. REPORT TYPE	3. DATES COVERED **00-00-2010 to 00-00-2010**
4. TITLE AND SUBTITLE **Using Polymer Electrolyte Membrane Fuel Cells in a Hybrid Surface Ship Propulsion Plant to Increase Fuel Efficiency**		5a. CONTRACT NUMBER
		5b. GRANT NUMBER
		5c. PROGRAM ELEMENT NUMBER
6. AUTHOR(S)		5d. PROJECT NUMBER
		5e. TASK NUMBER
		5f. WORK UNIT NUMBER
7. PERFORMING ORGANIZATION NAME(S) AND ADDRESS(ES) **Massachusetts Institute of Technology,77 Massachusetts Avenue,Cambridge,MA,02139**		8. PERFORMING ORGANIZATION REPORT NUMBER
9. SPONSORING/MONITORING AGENCY NAME(S) AND ADDRESS(ES)		10. SPONSOR/MONITOR'S ACRONYM(S)
		11. SPONSOR/MONITOR'S REPORT NUMBER(S)

12. DISTRIBUTION/AVAILABILITY STATEMENT
Approved for public release; distribution unlimited

13. SUPPLEMENTARY NOTES

14. ABSTRACT

An increasingly mobile US Navy surface fleet and oil price uncertainty contrast with the Navy's desire to lower the amount of money spent purchasing fuel. Operational restrictions limiting fuel use are temporary and cannot be dependably relied upon. Long term technical research toward improving fuel efficiency is ongoing and includes advanced gas turbines and integrated electric propulsion plants, but these will not be implemented fleet wide in the near future. The focus of this research is to determine if a hybrid fuel cell and gas turbine propulsion plant outweigh the potential ship design disadvantages of physically implementing the system. Based on the potential fuel savings available, the impact on surface ship architecture will be determined by modeling the hybrid fuel cell powered ship and conducting a side by side comparison to one traditionally powered. Another concern that this solution addresses is the trend in the commercial shipping industry of designing more cleanly running propulsion plants.

15. SUBJECT TERMS

16. SECURITY CLASSIFICATION OF:			17. LIMITATION OF ABSTRACT	18. NUMBER OF PAGES	19a. NAME OF RESPONSIBLE PERSON
a. REPORT **unclassified**	b. ABSTRACT **unclassified**	c. THIS PAGE **unclassified**	**Same as Report (SAR)**	**65**	

Using Polymer Electrolyte Membrane Fuel Cells in a Hybrid
Surface Ship Propulsion Plant to Increase Fuel Efficiency
by
Douglas M. Kroll

Submitted to the Department of Mechanical Engineering and Engineering Systems Division on May 7,
2010 in Partial Fulfillment of the Requirements for the Degrees of

Naval Engineer
And
Master of Science in Engineering and Management

Abstract

An increasingly mobile US Navy surface fleet and oil price uncertainty contrast with the Navy's desire to lower the amount of money spent purchasing fuel. Operational restrictions limiting fuel use are temporary and cannot be dependably relied upon. Long term technical research toward improving fuel efficiency is ongoing and includes advanced gas turbines and integrated electric propulsion plants, but these will not be implemented fleet wide in the near future.

The focus of this research is to determine if a hybrid fuel cell and gas turbine propulsion plant outweigh the potential ship design disadvantages of physically implementing the system. Based on the potential fuel savings available, the impact on surface ship architecture will be determined by modeling the hybrid fuel cell powered ship and conducting a side by side comparison to one traditionally powered. Another concern that this solution addresses is the trend in the commercial shipping industry of designing more cleanly running propulsion plants.

Thesis Supervisor: Mark S. Welsh
Title: Professor of the Practice, Naval Construction and Engineering

Thesis Supervisor: Pat Hale
Title: Director, System Design and Management Fellows Program

Acknowledgements

Table of Contents

List of Figures

List of Tables

Page Intentionally Left Blank

1. Introduction

Over the past decade the US Navy has expanded its mission from the traditionally defined role of maintaining a sea line communication presence to assisting in the global war on terror and other forward deployed operations. Over time this shift will require that surface ships and submarines are able to quickly relocate to a more loosely defined set of locations. One way this transition can be achieved is by adding to the total number of ship hulls in service as well as requiring that each individual ship transit for a larger portion of its steaming profile. Due to the extensive costs associated with designing, building, and manning new ship classes, increasing the number of in service hulls has been occurring slowly. Additionally, the unstable cost of fuel has made operating them with this level of flexibility more expensive.

1.1 Problem Statement

Two specific problems arise as the Navy requires a naval ship possess more mobility. The first is the operational cost associated with the higher overall fuel use. This cost is determined primarily by the price of oil which is driven by market supply and demand. The second is an indirect technical cost which is realized in maintaining an adequate hull form and displacement in spite of the larger required fuel storage volume. As a ship's displacement is increased, higher construction costs are immediately realized due to the larger quantity of fabrication material. Additionally, as displacement and submerged surface area becomes larger, an increase in the hull's frictional and formal drag raise the ships overall hydrodynamic resistance. This higher resistance must be overcome and can be represented as a decrease in propulsive efficiency, which then requires an even larger fuel storage volume.

Several viable options are available to deal with the trend of increasing required surface ship mobility. The first is to install a more robust military support infrastructure to ease forward deployed refueling. This would allow ships to travel less distance between refueling and the depots could obtain overseas oil without having to pay transportation costs. The disadvantages of this solution are that the fuel price is still driven by external factors, and processing the fuel would have to be paid for or conducted at the remote site.

Another method available would be to focus on technological advances which increase propulsive and electrical efficiency. This could be accomplished by advanced prime movers and motors such as high temperature superconducting motors, inter-cooled recuperated gas turbines, and an all electric based ship architecture. Although there is promise in reducing power losses based on ongoing research, these are not achievable in the near term and become expensive to implement once the technology does become mature.

The third potential solution for new ship designs is to use diesel generators in the place of gas turbines which are more fuel efficient in all loading conditions. One disadvantage is that diesel generator volume and displacement far exceed that of gas turbines. This means any fuel savings advantage which could lead to smaller ship displacement would be diminished by the larger weight requirements of the more bulky diesel powered prime movers. Another disadvantage of this solution is that with current diesel engine technology, a significantly higher amount of harmful effluent fumes are released compared to gas turbines.

A final solution available is to use an alternate propulsion source such as electromechanical fuel cells to either completely power or supplement currently installed gas turbines in meeting the ship's propulsion

requirement. This method is beneficial for several reasons. These types of electricity sources, in addition to being more efficient than gas turbines, operate with significantly fewer moving parts. Less parts leads to quieter and more reliable operation. These characteristics allow for efficient power but also assist the ship remain stealthy and ensure propulsion remains continuous. Both of these benefits contribute to the ship's overall survivability.

Although there are benefits, a problem arises while attempting to implement this solution within present day propulsion plant configurations. An efficient conversion process to couple dissimilar sources of prime mover energy and still allow for engine room flexibility is not yet available and electric motors in use do not possess the capability of simultaneously interacting with both an electric and mechanical power source. Because of this, complex mechanical linkages would be required to achieve the desired configuration, which drives up fabrication and maintenance costs.

Another disadvantage to fuel cells is obtaining the fuel source. Typical fuel cells are powered by hydrogen which must be either loaded directly from off hull sources or generated on board. As there is no hydrogen infrastructure in place it is assumed onboard reforming of gas turbine fuel would be required for any shipboard use of fuel cells in the near future.

1.2   Establishing Context

To lower its operational budget, the Navy has placed an emphasis on decreasing overall fuel use. However, this philosophy contradicts with missions which tend to increase a given hull's cumulative transit time. Due to these differing pressures, more efficient ship designs seeking to raise propulsion plant efficiency while at the same time meeting battle group speeds are highly desirable.

In addition to engineering improvements, a larger focus is being placed on lowering foreign oil dependency. This process once achieved will benefit the US Department of Defense by creating more stable fuel pricing. Until the US implements steps to make this occur however, the Navy will go through periods where prices rise uncontrollably and operational tradeoffs will have to be made to remain financially responsible. Steps toward this goal will take time making it a long term process. Any factors that can quickly mitigate excessive fuel consumption are therefore urgently needed.

Another consideration which makes addressing this problem urgent is that commercial shipping regulations are becoming more restrictive toward ensuring cleaner running ships are designed and operated. Many recently implemented laws are aimed at reducing or eliminating completely the release sulfur, carbon monoxide, and other harmful propulsion plant effluents. Any long term shifts in US Navy propulsion plant acquisition will most likely need to address environmental concerns to stay in step with industry standards.

1.3   Complications of Implementing Cost Reductions

The problem of Department of Defense cost overruns is not new and has in the past been engaged at both the acquisition and operational level. To lower fuel costs, solutions such as manually restricting speed and monitoring fuel use have been proposed and in some cases implemented. These measures however do not address the underlying problem of ships that are designed for high speed operation but have poor fuel efficiency at low speeds. These fixes are also short term solutions which tend to be responsive in nature and will not continue to provide benefit as operational constraints change.

The difficulty in implementing tangible solutions is that decision making within the design process is very political. Current spending habits are engrained. A high level of ship performance and component level

technological advance has also been deemed acceptable in new construction projects. This leads to ship operational requirements which drive the ship to perform a broad range of functions well. For example, having a large number of ship classes required to meet aircraft carrier battle group speed regardless of ship type, displacement or primary mission. This has led to the higher fuel consumption gas turbines being more prevalently selected within ship designs due to their high performance level.

1.4 Research Proposal

The focus of this research is to determine if an optimized propulsion plant utilizing the fuel savings of a hybrid fuel cell and gas turbine propulsion engine outweigh the potential ship design disadvantages of physically implementing the system. My intention is to categorize three possible fuel cell types to highlight their advantages and disadvantages. Inherently driven inefficiencies as well as durability issues will also be discussed. This will allow the development of an accurate voltage-current relationship over the possible fuel cell operating power levels. Using this background information, one fuel cell type will be selected and developed further for a specific shipboard application. Once the parameters and assumptions are determined for the fuel cell of interest, an optimizing program will be generated using MATLAB®. This program will analyze a family of notional hybrid propulsion plants across a given spectrum of operational profiles and compare the potential fuel consumption to currently seen levels.

Finally, I intend to implement the optimized solution for hybrid fuel cell capacity at a total ship design level. Based on the potential fuel savings available I will qualitatively determine the impact on surface ship architecture by modeling the hybrid fuel cell powered ship and conducting a side by side comparison using the Advanced Surface Ship Evaluation Tool (ASSET®) version 5.3.

2.   Fuel Cell Discussion

Describing the general electric chemical reaction is the first step toward deciding if fuel cells as an alternate energy source can be feasibly implemented within a naval engineering application. Once the basis for operation has been established, the inherent electric losses which determine the voltage to current relationship will be identified and described. Next, the advantages and disadvantages of three prominent fuel cell types will be highlighted, with the most applicable selected for implementation analysis. Finally, several durability concerns of the desired fuel cell type, and how they may hinder implementation will be identified.

2.1   Electrochemical Reaction Description

Fuel cells generate electricity by using fuel in gaseous form to create a triple phase boundary, shown in Figure 1, which consists of fuel, electrolyte, and electrode. When this occurs, the heterogeneous oxidation process removes electrons from the charge carrier. The fuel after having been activated, transfers free electrons to the electrode across the catalyst while the charge carriers are driven into and across the electrolyte.
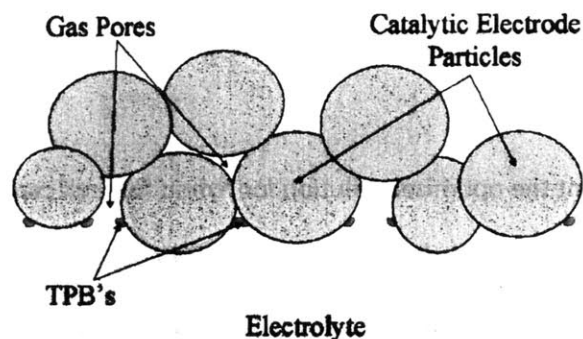
Figure 1: Fuel Cell Triple Phase Boundary (O'Hare, 2009)

The oxidation reaction can occur with multiple fuel source and electrolyte material combinations which are capable of stripping electrons from the base compound. A typical oxidation reaction with hydrogen as the fuel is shown in Equation 1.

$$H_2 \rightarrow 2H^+ + 2e^-$$

Equation 1: Oxidation Reaction

Once fuel activation has occurred, the total number of electrons and activation site surface area determine the maximum available current. The surface area is fixed by the physical design of the electrolyte electrode interface, which can be designed and therefore customized for a given application. The total number of electrons however is driven by the concentration of fuel accessing the interface. This concentration is determined by the type of fuel, and flow rate across the boundary. Although these characteristics are also constrained by design, to achieve a stable power level, fuel concentration must be maintained by either an automatic flow control system or meticulous operator control. Fuel that is not activated is cascaded away from the anode and may either activate at a farther downstream triple phase boundary location, or be pushed eventually to the exit of the fuel cell. This makes adequate flow control extremely important to maintaining a high level of efficiency.

After the electrons and charge carriers have reached the fuel cell outlet location they are recombined at another triple phase boundary using a cathode and reactant. With oxygen as the reactant, recombination creates water according to the basic reduction reaction shown in Equation 2.

$$O_2 + 4H^+ + 4e^- \rightarrow 2H_2O$$

Equation 2: Reduction Reaction

Because the overall reaction is a thermodynamically favorable electron process and not a chemical reaction, interactions occur without a release of free charge but produce heat, pure water, and power in

15

the form of electric current, as shown in Figure 2. This dictates that the reaction rate efficiency is limited by the amount of energy required to cause activation, recombination, and overcome several other inherent kinetic losses which are discussed in chapter 2.2.
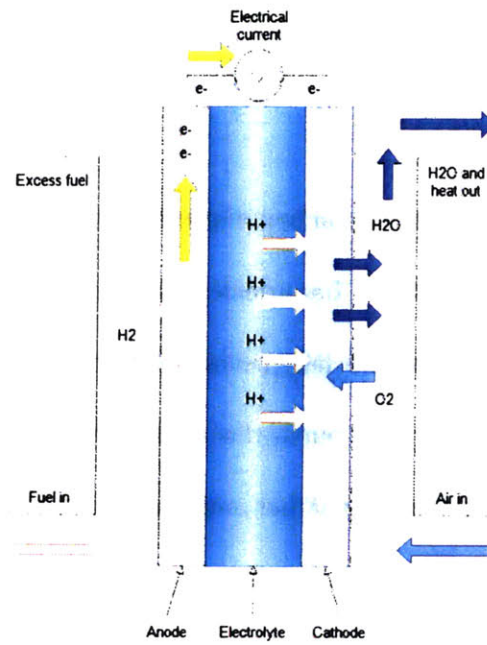
Figure 2: Fuel Cell Flow Paths (O'Hare 2009)

2.2   Inherent Fuel Cell Losses

Using the oxidation and reduction equations shown in chapter 2.1, the available electric potential for a fuel cell utilizing pure hydrogen is bounded by the idealized Gibbs free energy of 1.23 volts. When fuel cell kinetic limitations are levied on the system however, irreversible losses lower this value. The three major categories of losses which are all described here are:

1)   Activation losses driven by the electrochemical reaction and cell composition

2)   Ohmic losses affecting both ionic and electron conduction

3)   Concentration losses due to mass transport inefficiencies

The first type of irreversible fuel cell losses are activation losses. These losses are most significant at low

current densities, but tend to stabilize once a large enough current density has been developed as

shown in Figure 3.
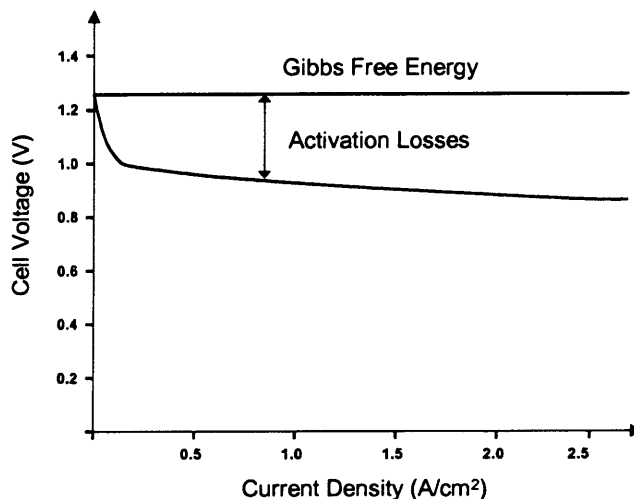
Figure 3: Fuel Cell Activation Losses

Activation losses affect low current operations because of how the fuel cell operates when it first comes

into contact with fuel. When initially supplied with hydrogen at the anode and oxygen at the cathode,

the system attempts to naturally balance the chemical reaction rate. Both oxidation and reduction

reactions are free to occur simultaneously in the forward and reverse directions as triple phase

boundary points are exposed to reactants. Initially the forward reaction rate at both electrodes is larger

due to the electrical and chemical differential. Once the electric and ionic charge has built up on the

electrode and within the electrolyte, the system has reached electrochemical equilibrium. This level is

the Galvanic charge. With the system in equilibrium, further forward reactions are now no longer

possible meaning no useful current is yet available. To forward bias the fuel cell and derive electric

power, a decrease in cell voltage must be induced. This in effect drives the chemical reaction to the

forward direction, but becomes a direct loss on output power.

These losses can be mitigated though the selection of fuel cell material including to a large extent the type of catalyst selected. This occurs because a catalyst, platinum for example, makes the electrons more likely to break away from the fuel when it comes into contact with the electrode, so the electrochemical equilibrium occurs more easily. This effect can be recognized as a decrease in the activation energy plateau, meaning a smaller decrease in electric potential must be induced to forward bias the cell. During operation maintaining adequate activation energy plays a key role in developing the voltage current relationship.

Ohmic losses are the second type of irreversible fuel cell losses, which are a linear function of current. Because electron transport is driven by a voltage gradient across the electrode, and hydrogen ionic transport is driven by both voltage gradient and chemical diffusivity through the electrolyte, any resistance to these flows will take away from the efficiency of the fuel cell. The losses exhibit a linear shape across the useable current ranges as shown in Figure 4.
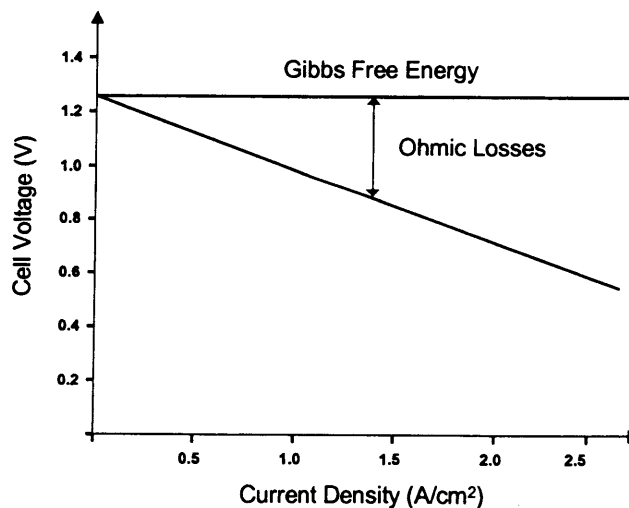
Figure 4: Fuel Cell Ohmic Losses

Fuel selection and operational conditions such as temperature, atmospheric pressure, and humidity affect the magnitude of ohmic losses. They are most dependant however on the amount of fuel cell

loading. Designers ultimately manage ohmic losses in the operational current regions through design considerations to reduce the electric resistance of the fuel cell electrodes while the ionic conductivity properties of the electrolyte are increased.

The final type of irreversible fuel cell losses considered here are concentration losses. The basis for these losses are fuel transport inefficiencies, which leave the fuel cell either underpowered by not supplying enough fuel, or lead to inefficient use as too much fuel becomes exposed to the entire region of triple phase boundaries leaving fuel unused. To combat these losses designers can choose to install a constant stoichiometry flow control. Additionally, pure oxygen can be selected as the reactant vice air. This characteristic implies that for a given fuel cell design, efficient use in the respective high current region is severely limited. The impact concentration losses have on fuel cell performance is shown in Figure 5.
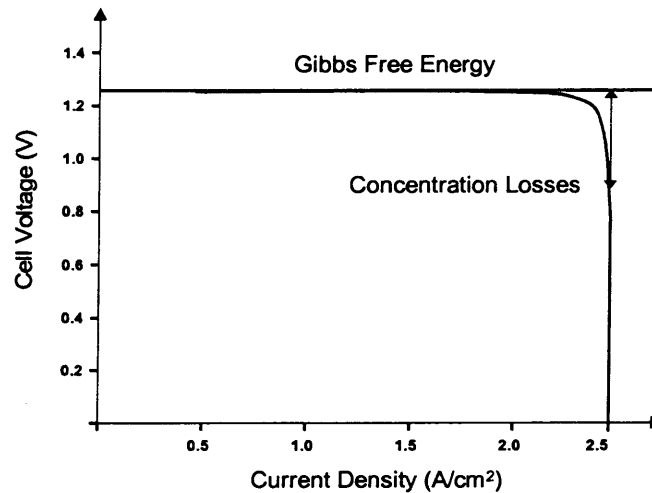
Figure 5: Fuel Cell Concentration Losses

Once all the categories of losses are considered, the fuel cell's voltage to current profile is developed by lowering the Gibbs free energy at each respective current as shown in Figure 6.
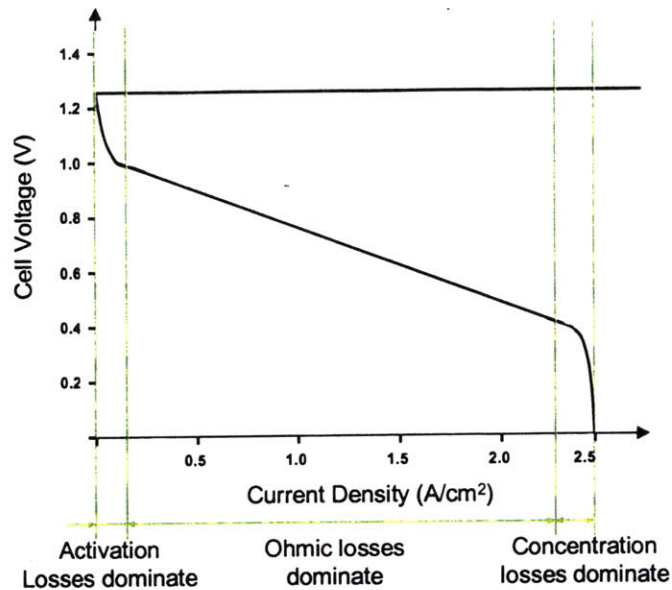
Figure 6: Fuel Cell Voltage Current Relationship with Irreversible Losses

This nonlinear relationship is characterized by the Butler-Volmer relationship and can be used to determine fuel cell performance under a wide range of loading and atmospheric conditions. One advantage from a design perspective to quantifying how the electrochemical reaction rate affects ultimate fuel cell operation is that output performance becomes an extremely controllable process. Because the factors which limit this rate have been meticulously characterized in industry, the efficiency of multiple types of fuel cells is also known. This means that simple design modifications can be readily implemented where feasible to improve kinetic performance including:

1) Increasing reactant concentration or using pure oxygen

2) Decreasing activation barrier by catalyst selection based on the operating environment. For example, selection of a platinum catalyst for use within a low temperature fuel cell, or nonprecious metal conductors for use at higher temperatures.

3) Increase fuel cell operating temperature which increases ion conductivity and fuel mass transport

4)   Increase the number of reaction sites by creating roughness in the interface region

2.3   Types of Fuel Cells

Fuel cells are distinguished by the chemical reactions which occur at both the oxidation and reduction triple phase boundaries. By selecting an applicable fuel source and electrolyte material, the fuel cell components and operational conditions required to achieve optimal performance generally become fixed. This implies that although multiple combinations of fuel cell components capable of producing usable current exist, only a few configurations are preferable and warrant discussion. The three considered for this research are the solid oxide fuel cell (SOFC), the polymer electrolyte membrane fuel cell (PEMFC), and the phosphoric acid fuel cell (PAFC).

2.3.1   Solid Oxide Fuel Cells (SOFC)

The first type of fuel cell considered is the SOFC. This fuel cell utilizes a solid oxide electrode which is typically constructed of yttria-stabalized zirconia and operates at temperatures of 600°F to 1000°F. Although these fuel cells possess a desirable operating efficiency, their relatively high operating temperatures require significant heat removal or cogeneration support systems, and drive up the cost as temperature resistant components are required.

The major advantage of the SOFC operating temperature range is that inherent losses are reduced and the fuel cell functions at a high efficiency. The temperature range also allows for selection of a non-precious metal catalyst. Adding this type of selection flexibility mitigates some of the cost associated with a more robust design and manufacturing requirement, as well as adds significant poisoning resistance.

Another advantage of the SOFC is that it operates with a high level of fuel selection flexibility. If onboard reformation of diesel generator or gas turbine fuel is not the most practical method of producing an acceptable reactant, the SOFC can readily be supplied with another more accessible fuel with only minor adjustments to the overall component architecture and support systems.

The main problem for implementing SOFC systems onboard surface ships is that materials which come in contact with high temperatures must be precisely designed and manufactured. This concern makes fabrication expensive and creates thermal cycling difficulties. To ensure each component's structural integrity is in fact maintained, the start up and operational cycling rates must be strictly regulated. Additionally, selecting the thickness of the electrolyte becomes problematic. To ensure ionic transport is not impeded, the electrolyte must be as thin as possible. To maintain structurally integrity for meeting durability concerns however, the thickness must be increased. This contradiction means a SOFC may have either performance or durability issues for use within a given application.

2.3.2   Polymer Electrolyte Membrane Fuel Cells (PEMFC)

The PEMFC operates by passing hydrogen that has been stripped of its electrons through a perfluorinated polymer. Electrons which have been removed from the fuel then bypass the electrolyte according to the process and reactions described in chapter 2.2. This configuration permits operation at extremely low temperatures compared to other fuel cells.

Some advantages of PEMFC operating at such low temperatures is that the fuel cell doesn't require as meticulous of a support system infrastructure which allows the fuel cell to be packaged in a compact manner. This makes the PEMFC extremely scaleable when space and volume limitations are not strict. In addition to these characteristics, the key benefit to PEMFCs from a naval architecture perspective, as

previously described, are their lack of moving parts, and ability to produce only useable electricity and pure water.

Because of the fuel cells low operating temperature requirement and the proton conducting ability of the polymer membrane, electrolyte thickness can be as low as 20 μm, which significantly decreases ionic conductivity losses. "The PEMFC currently exhibits the highest power density of all the fuel cell types (300-1000 mW/cm^2)." (O'Hare, 2009 p. 264) Additionally, PEMFCs are able to quickly start and cycle across useable current levels, making it operationally flexible. One final advantage of using PEMFCs over other types is that current research employed by auto manufacturers is focused on component level upgrades that will tend to raise overall system level reliability, as well as increase operating efficiency even further.

Although the PEMFC possesses attractive operating properties, there are several disadvantages to overcome when considering them as a valid power source. The first is that the low temperature requires a platinum catalyst to mitigate activation losses, which drives up construction costs and create specific durability concerns. The system is highly susceptible to carbon monoxide and sulfur poisoning. After operational periods where fuel cell components are exposed to these fuel byproducts, performance decreases, and the potential for catastrophic failure of either the electrolyte or some other component becomes real. The reason this disadvantage is even more applicable within naval applications is because onboard reforming of either diesel or gas turbine fuel must be used, which both have high concentrations of sulfur.

Another disadvantage is that by selecting perfluorinated polymer as the membrane material, an active water management system must be designed and implemented in order to maintain the electrolyte's

23

integrity. If the membrane becomes damaged due to an improper water level, the fuel cell will in effect short circuit. This occurs because hydrogen molecules at the anode are allowed to directly interact with the cathode, which transfers electrons around the electric load instead of through it. Both of these disadvantages must be taken into consideration if an appropriate surface ship propulsion system is to be designed using PEMFCs.

2.3.3 Phosphoric Acid Fuel Cells (PAFC)

The final type of fuel cell considered uses a phosphoric acid electrolyte in liquid form. This is accomplished by maintaining a reservoir of H_2PO_4 electrolyte material between two graphite electrodes. Due to the chemical characteristics of the electrolyte, the operating temperature of the fuel cell must be maintained between $100°F$ and $400°F$. This fuel cell configuration, similar to PEMFCs, transfers protons across the electrolyte which means it follows the anode and cathode reactions and limitations described in chapter 2.1.

The primary advantages of this technology are that it is mature and currently employed in land based utilities as both primary and backup power sources. Because the operating temperature is slightly higher than a PEMFC, the efficiency is slightly higher but without all of the temperature dependant disadvantages seen in with the SOFC configuration.

A significant detractor toward putting PAFCs onboard surface ships is that the electrolyte is extremely corrosive and must be constantly monitored and replenished during operation. This requires that ship designers put appropriate storage and handling considerations into place.

2.4   Fuel Cell Selection

The advantages and disadvantages of the three fuel cell types are summarized in Table 1.

Fuel Cell Type	Advantages	Disadvantages
SOFC	-Fuel Selection Flexibility -Nonprecious metal catalyst -High power density	-High temperature material issues -Rigorous support system requirements
PEMFC	-Good start stop capability -Low temperature operation -Scalable power levels	-Platinum catalyst -Polymer membrane expensive and has potential for damage -Susceptible to CO and S poisoning
PAFC	-Mature technology -High reliability -Low cost electrolyte	-Corrosive liquid electrolyte -Platinum catalyst -Susceptible to CO and S poisoning

Table 1: Fuel Cell Characteristics Comparison (O'Hare 2009)

Although they are a well researched technology, due to the low flexibility and rigorous support system requirements, the SOFC is not the most favorable selection for a naval application. When considering a PAFC for use within a naval architecture application, the additionally required corrosive material measures to support the phosphoric acid electrolyte, as well as the disadvantages already seen by PEMFCs of susceptibility to carbon monoxide and sulfur poisoning make this type generally less desirable than PEMFCs.

2.5   Durability Concerns

Durability is one additional hurdle to be overcome before the PEMFC can be confidently used in a naval engineering application. To provide reliable power for the ships service electric plant and propulsion, the fuel cell and all of its supporting equipment must run for a large number of hours at the expected performance level. The multiple failure mechanisms leading to a power drop off, as well as any gradual performance degradations due to individual component malfunctions or improper operation must be

fully understood and ultimately controlled before fuel cells will serve as a realistic means of shipboard power generation. As a final design consideration, the fuel cell must be designed in such a manner to compensate for any expected life cycle degradations.

The first area that failure can occur in a fuel cell is across the electrolyte. Because of the possibility for extremely thin membranes in the PEMFC it becomes an even more real concern. The electrolyte is susceptible to harmful mechanical interactions consisting of foreign material or substances from preexisting flaws which become worse and damage the physical membrane. Because electrolytes are designed to attract ions so readily, chemical and ionic attacks are another likely cause of degradation. This is due to chemicals in the form of caustic free radicals and other harmful ionic contaminants become absorbed and performing unpredictable wear and damage.

The second area that is highly susceptible to durability issues within the PEMFC is the electrode catalyst boundary. A fuel cell's output power is a function of electrode surface area, which determines the rate at which electrons can be in effect absorbed from the fuel into useable current. Multiple chemical processes such as platinum pitting, oxidation, and dissolution, tend to decrease that surface area and will over time lower total cell efficiency. This implies that after platinum degradation has occurred, a higher amount of fuel will be required at the respective triple phase boundary to sustain the electrochemical rate that the same fuel cell experienced earlier in its life.

There are still many challenges toward understanding each failure mechanism and how it relates to overall fuel cell kinetics. The advantage for naval engineering however is that knowledge can be leveraged from the automotive industry, which has set future performance and reliability goals for the PEMFC. Automotive applications are similar in that although the power required to supplement

shipboard propulsion is several magnitudes of order larger, the operational profile is similar between the two applications. Car power sources must be able to start quickly from a cold condition as well as operate in either a stop and go fashion or produce a sustained power level for a given period, and perform at power for a comparable life cycle. Until PEMFC reliability thresholds have been proven in less than ideal atmospheric conditions, even though fuel cell possess desirable powering and efficiency characteristics, they will not be acceptable for shipboard use.

3.   Propulsion Plant Model

Now that fuel cells as an alternate power source and PEM fuel cells in specific were selected as a desirable alternative power source for use within a hybrid surface ship propulsion plant, a propulsion plant optimization model was developed. The goal of the model was to determine the amount of fuel cell power that should be installed on a surface ship application to derive the largest decrease in fuel consumption. The program also determined how best to operate those fuel cells in concert with gas turbines.

Describing the optimization model is conducted in two steps. The first is the set of specific assumptions which were made with respect to the desired propulsion plant and ship operational characteristics. The second is the general flow based algorithm, and resulting MATLAB® code.

3.1   General Assumptions

Several general assumptions were made to assist in developing the code algorithm. These assumptions fed the model by constraining inputs and served to conservatively bind the optimization program.

3.1.1 Gas Turbine Inputs

The first assumption was that a DDG-51 flight 1 US Navy destroyer is the ship under analysis. This decision led to the first input, which is that the propulsion plant for comparison is outfitted with 4 LM-2500 gas turbines dedicated to developing speeds of 35 knots through a mechanical drive propulsion system.

The next input required by the program is the useable gas turbine power range. Because all 4 turbines are capable of producing power in concert and each is capable of developing 25 MW of comparable electrical power, the range of powers to be analyzed is up to 100 MW. This will serve as the maximum value for iteration when propulsion plant loading is considered by the model.

Another assumption is that the specific fuel consumption extends continuously across all possible loading states of the prime mover but is nonlinear. A fuel consumption curve used by this model was developed by scaling a general gas turbine consumption curve in to the 25 MW limit, shown in Figure 7.
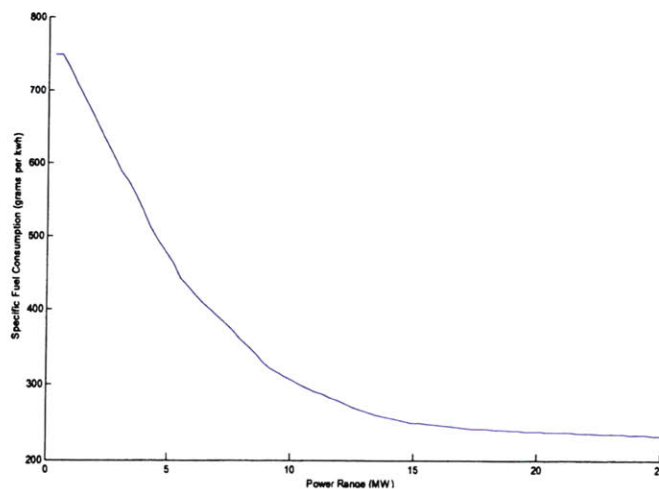
Figure 7: Gas Turbine Specific Fuel Consumption (Woud, 2002)

Based on the shape of the specific fuel consumption curve and some additional analysis, the next assumption pertains to how the gas turbines are loaded. It is seen from the two total fuel consumption curves in Figure 8 that for a majority of the desired power ranges, the optimal fuel efficiency at a given load is achieved when gas turbines are operated sequentially. This occurs because bringing multiple gas turbines online in a parallel fashion keeps each one operating at a much lower power level forcing the specific fuel consumption of each higher.
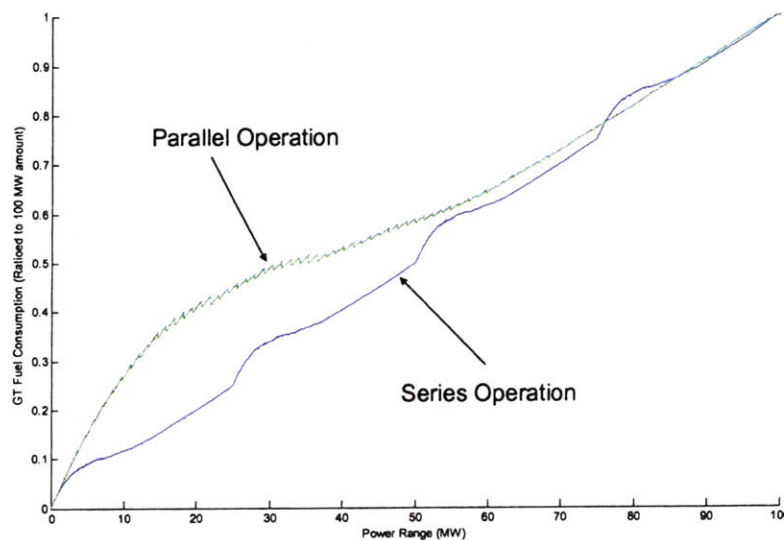
Figure 8: Total Fuel Consumption of 4 Gas Turbines

This assumption affects the optimization model as any benefit from adding fuel cells to the propulsion plant must be shown when compared to the best possible fuel consumption, which occurs under 4 gas turbine series operation. For loading purposes, all required power below 25 MW will be assumed by one prime mover. Another gas turbine will then be brought online to accept additional power requirements, while the original gas turbine continues operating at full load. Although this is not the traditional operating pattern based on the current US Navy fleet tendency of having all gas turbines lightly loaded to provide high speeds in a short notice, this process produces the best possible fuel use profile which will be benchmarked.

Evaluating the fuel consumption differential curve in Figure 9, the gas turbine operating method assumption can be seen as valid for all values with the exception of powers between 75 – 85 MW. The overlap in this segment is due to the starting cycle of the final gas turbine as it picks up load just over the 75 MW value. This forces it to operate at a very high specific fuel consumption, while the 4 gas turbines in parallel are by this point operating at more than 75% of their rated load. It is assumed that the magnitude of the fuel consumption represented by the overlapping section is small and series operation will be considered here.
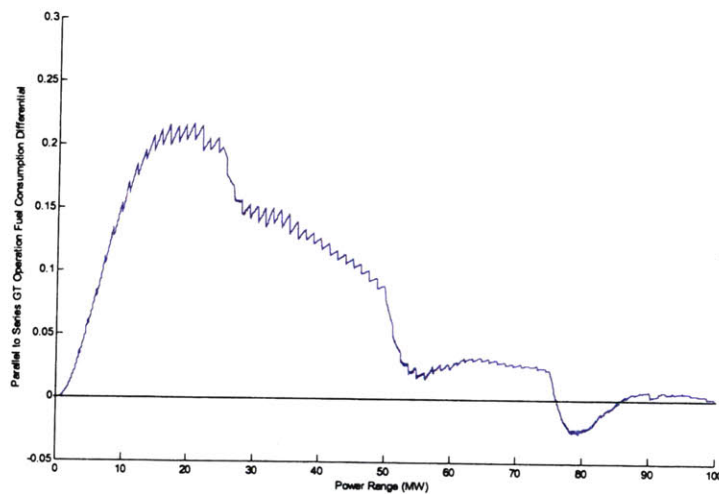
Figure 9: Fuel Consumption Differential Based on Operating Method

A corollary assumption concerning gas turbine operation was that even though they operate more efficiently under higher loading, it is not beneficial to overload a gas turbine in hopes of achieving lower fuel consumption by decreasing the prime mover's specific fuel consumption. Because the shape of the gas turbine total fuel consumption curve does not experience a negative slope across any two power ranges, it is most conservative for fuel usage to exactly load the prime mover at a desired level. This is seen discretely in Figure 10. If only 5 MW of power is desired, a single gas turbine should not be operated at 10 or 15 MW.

30
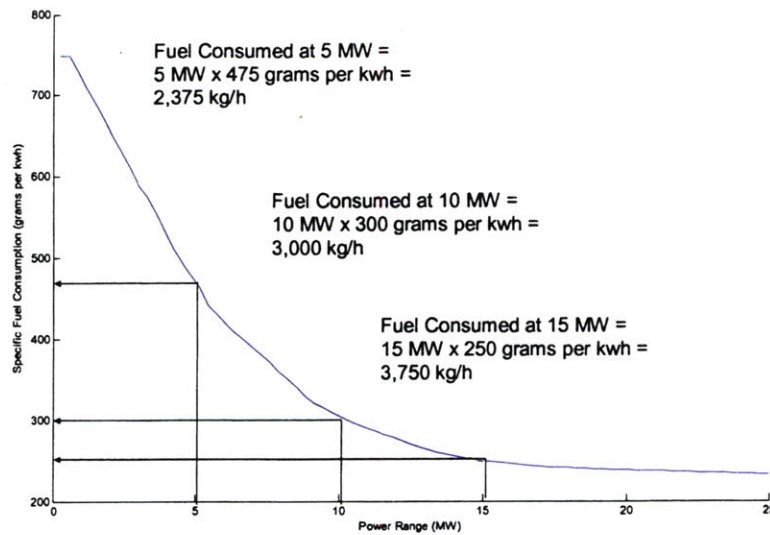
Figure 10: Gas Turbine Fuel Consumption at 3 Loading Conditions

3.1.2 PEMFC Inputs

Once assumptions and inputs for gas turbine operation were determined, identifying how the PEMFC operates in the hybrid propulsion plant was accomplished. The first assumption in this area is that blocks of 250 kilowatt PEMFCs will be installed and operated with an automatic fuel control system. The propulsion plant will iterate from 1 to 40 of the fuel cells which allows up to 10% of the total required propulsion load to be powered either partially or fully from the alternative power source.

To ensure even wear on fuel cell components, all installed fuel cell blocks are to be loaded to their desired power level simultaneously. This assumption is valid from a fuel consumption perspective as efficiency is linear when a family of fuel cell voltage to current curves is analyzed, shown in Figure 11.
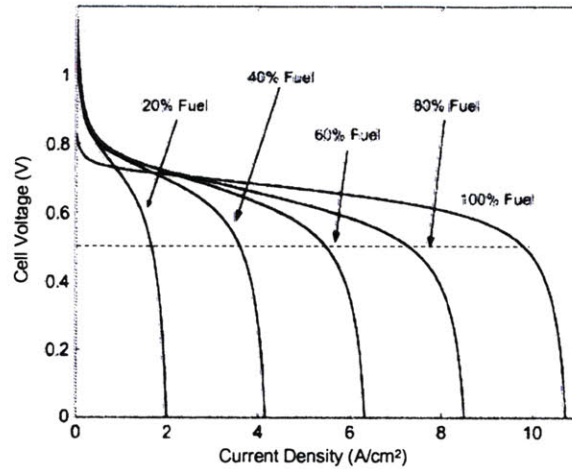
Figure 11: Fuel Cell Voltage Vs. Current Density

Using values in the plot provided, the power density can be seen as a linear function of the fuel rate

shown in Table 2.

Fuel Rate (% flow)	Cell Voltage Volts	Current Density A/cm2	Power Density Watts/cm2	Power Density / Fuel Rate
20	0.5	1.9	0.95	4.75
40	05	3.8	1.9	4.75
60	0.5	5.7	2.85	4.75
80	0.5	7.6	3.8	4.75
100	0.5	9.5	4.75	4.75

Table 2: Fuel Cell Operating Parameters

For controlling the fuel cell, it was assumed that an accurate fuel control system was available and could

accurately control power output in 2.5 kilowatt increments, or 1% of total fuel cell output power. To

adjust for the finite timing and accuracy limitations that exist in current PEM fuel cells, 10% degradation

to the assumed efficiency was inserted to add a level of conservatism. Fuel consumptions of 250 grams

for each kilowatt hour could be seen in a real world application. With the efficiency decrease

implemented however, selection of PEM fuel cells in their current state yield a power source operating at an efficiency of 275 grams of fuel for each kilowatt hour.

3.1.3 DDG-51 Flight 1 Inputs

The final set of assumptions has to do with the naval architecture application. The DDG-51 Flight 1 hull requires a certain thrust to achieve a given speed. These values are known and are given for usable speeds in Figure 12.
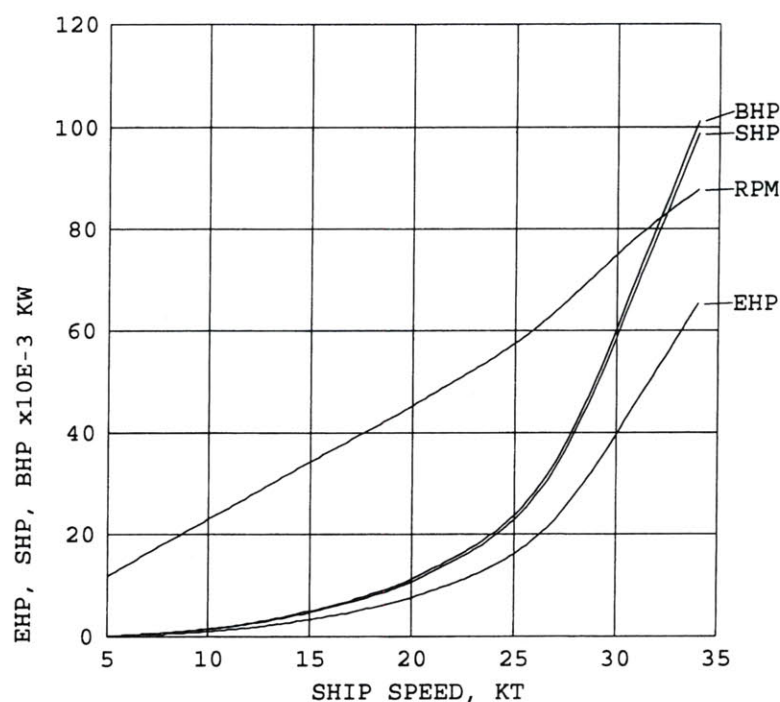
Figure 12: DDG 51 Flight 1 Powering Curve

The final assumption is that a discrete speed profile will be used. This assumption is valid because in typical operating conditions, engine orders are applied in standard bell formats. For example an all-ahead 1/3 or full bell correspond to exactly 5 or 20 knots. The profile to be used by the optimization model is generated in the ASSET® 5.3 surface combatant mission speed probability array and is identified in Table 3.

Speed (Fraction)	Speed (Knots)	Probability
$0.167 * V_{sustained}$	5	0.119
$0.500 * V_{sustained}$	15	0.466
$0.667 * V_{sustained}$	20	0.356
$0.833 * V_{sustained}$	25	0.044
$1.000 * V_{sustained}$	30	0.015

Table 3: DDG-51 Flight 1 Mission Speed Profile

3.2 Model Algorithm and code

Although developing the algorithm was an iterative process, the final version was completed after all of the general assumptions and inputs were made. This version, shown in Figure 13, identifies the desired order and progression of the program.
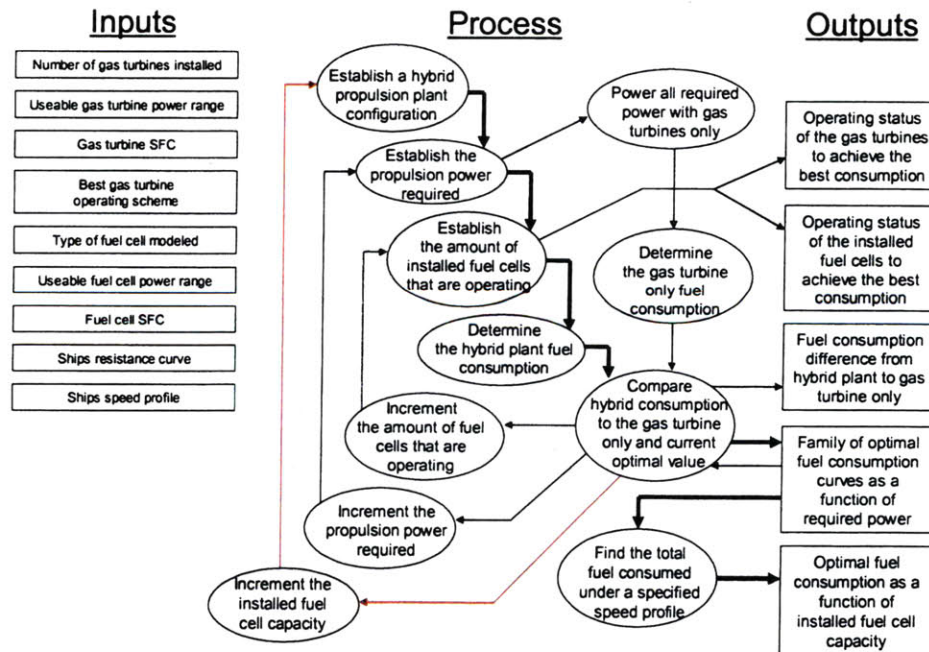
Figure 13: Propulsion Plant Optimization Algorithm

Determining the minimum fuel consumption during a DDG-51 underway as a function of number of installed fuel cells was the ultimate goal of the optimization program. Achieving this was accomplished by first establishing and iterating the states of three program variables, identified on the top left in the algorithm process section.

The first program variable, and where the model begins, is used to increment the amount of fuel cell capacity installed within the hybrid propulsion plant configuration. This variable has the most significant ramifications on the overall naval architecture of the ship design. This occurs because the required support and control systems for the fuel cell, as well as the physical block of fuel cells all take up propulsion plant surface area. They also add a large amount of weight to the ship's propulsion spaces. Although it has not yet been shown as a feasible quantity from an installation and operation perspective, it was assumed that up to 10% of the ships propulsion requirement could be assumed by fuel cells. This assumption requires the fuel cell capacity variable to iterate 40 times, increasing by one until all 40 configurations have been evaluated. Taking the range into consideration, and based on the optimization model's results, a value for the installed capacity will ultimately be selected and a total ship design will be developed and briefly analyzed for technical feasibility.

The second variable introduced and required for optimizing fuel consumption was propulsion power. This value was iterated from 0 to 100 MW in 100 kilowatt increments for each of the possible propulsion plant configurations, with 100 MW being the power required to propel the ship to near 35 knots. Although this power level is currently achieved by the four LM-2500 gas turbines, if any power can be more efficiently met at a lower fuel consumption rate with partial load taken by the fuel cells it needs to be considered by the model.

The third variable was used to set the operating status of the installed fuel cell capacity. This is necessary because even though a fixed fuel cell configuration is previously established and placed under load, the model should not be constrained into having to operate the fuel cells at 100% of their rated capacity for a given propulsion plant loading requirement. Iterating this quantity was done in 1% fuel cell increments, or 25 kilowatts. The operating status will ultimately be selected which performs at an overall lower fuel consumption compared to others, including the gas turbines only value. Although multiple operating conditions could exist for a given propulsion plant configuration and load that each consume the same amount of fuel, the one with the lowest number of operating fuel cells will be chosen.

The next function of the optimization model after the state of each of the three variables has been established is to determine the overall fuel consumption of the hybrid propulsion plant. This value was determined in a three part summation equation. The first part sums the fuel consumed by all fully loaded gas turbines, which is the product of the number of fully loaded turbine sets, gas turbine power range, and the specific fuel consumption of the gas turbine at its fully loaded state. The second part is used to determine and sum the fuel consumed by the installed fuel cells. This is found by determining the product of operational fuel cell capacity and fuel cell specific fuel consumption at the respective power level. The final segment in the fuel consumption equation is that which is assumed by a partially loaded gas turbine. To get the amount of power that is in a partially loaded state, the power assumed by fully loaded gas turbines and operating fuel cells is subtracted from the total power required. This partially loaded quantity is then multiplied by the specific fuel consumption of the gas turbine while operating at the appropriate ratio of its full load.

Once fuel consumption is found it is compared to the gas turbine only as well as the current optimal value, and a new optimal value is potentially set. The routine then continues iterating until it has evaluated all program variable combinations. After all states have been examined, a family of optimal fuel consumption curves as a function of required power is output for each of the installed hybrid plant configurations. These consumption curves are then converted based on the ships speed profile and resistance curve into an overall fuel consumption which is now only a function of installed fuel cell capacity.

4. Optimization Results

Once the optimization model was translated into MATLAB® code, the outputs defined in chapter 3.2 were generated. This chapter explains those results, as well as highlights the potential reasons for any trends or unexpected outcomes. There is also a sensitivity analysis conducted on the model parameters for speed profile and fuel cell specific fuel consumption.

4.1 Model Output

The first output from the model is the family of total fuel consumption curves, which are functions of required propulsion power. Each curve in the figures below represents a different propulsion plant configuration, from 1 to 40 fuel cells installed. The plot in Figure 14 shows required power up to 10 MW.
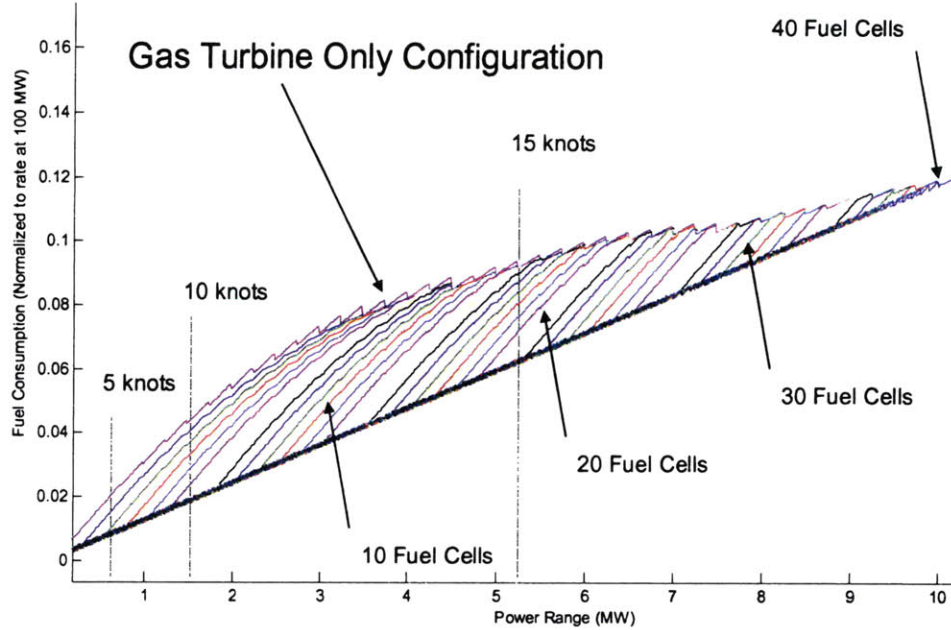
Figure 14: Total Fuel Consumption up to 10 MW

The figure also displays the gas turbine only curve, which represents the baseline propulsion plant with no fuel cell capacity installed. This gas turbine only curve serves as a de facto ceiling for optimized fuel consumption as any regions of required power where the best fuel efficiency is available with only gas turbines should be fulfilled with this operating method. In these scenarios, regardless of the installed fuel cell capacity, the operating status of all fuel cells will be to the off position. Another plot of total fuel consumption for up to 100 MW is displayed in Figure 15. The discrete speeds considered by the ship speed profile are noted on this total fuel consumption plot as well.
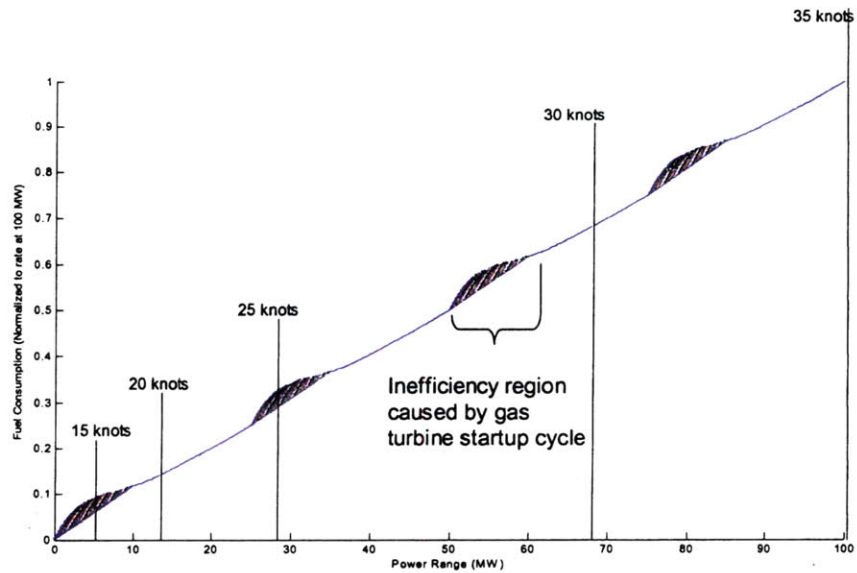
Figure 15: Total Fuel Consumption up to 100 MW

This curve shows that there are 4 finite regions within the power range domain where the gas turbines operating alone produce a relative inefficiency. Using both the 10 MW and 100 MW plots, a total of four out of the seven nominal engine order speeds are seen to fall within these regions. This implies that installing fuel cell capacity will reduce overall fuel consumption to the extent that these speeds are favored over speeds not within the inefficiency regions.

The next output from the optimization model is the difference in total fuel consumption between the gas turbine only curve and each of the 40 hybrid plant curves. The difference curves show that the regions along the power domain where fuel cells provide a consumption benefit are in fact discretely located. Each difference peak increases rapidly and drops after several megawatts of load have been placed on the partially loaded gas turbine, shown for a single pulse in Figure 16.
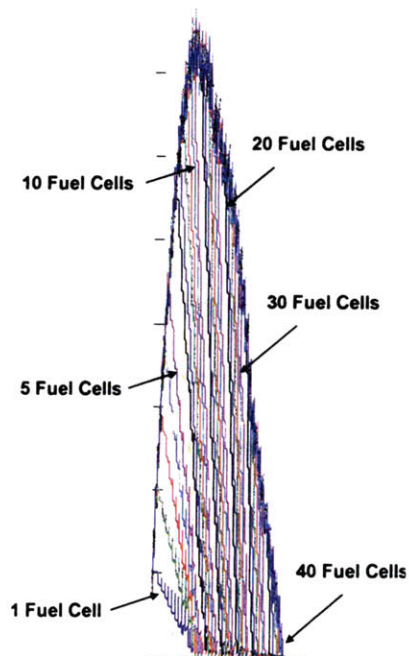
Figure 16: Fuel Consumption Differential for a Single Inefficiency Region

This fuel consumption difference curve is also shown in Figure 17 across the entire 100 MW region as a family of curves for each of the 40 propulsion plant configurations. The four pulses are seen to start coincident with each of the four gas turbine startup cycles as expected. They then taper off in favor of the gas turbine only profile when about 10 MW of load is able to be placed onto a partially loaded gas turbine. This process is seen to correlate with the gas turbine specific fuel consumption reaching the much lower slope in Figure 7 of Chapter 3.1.1.
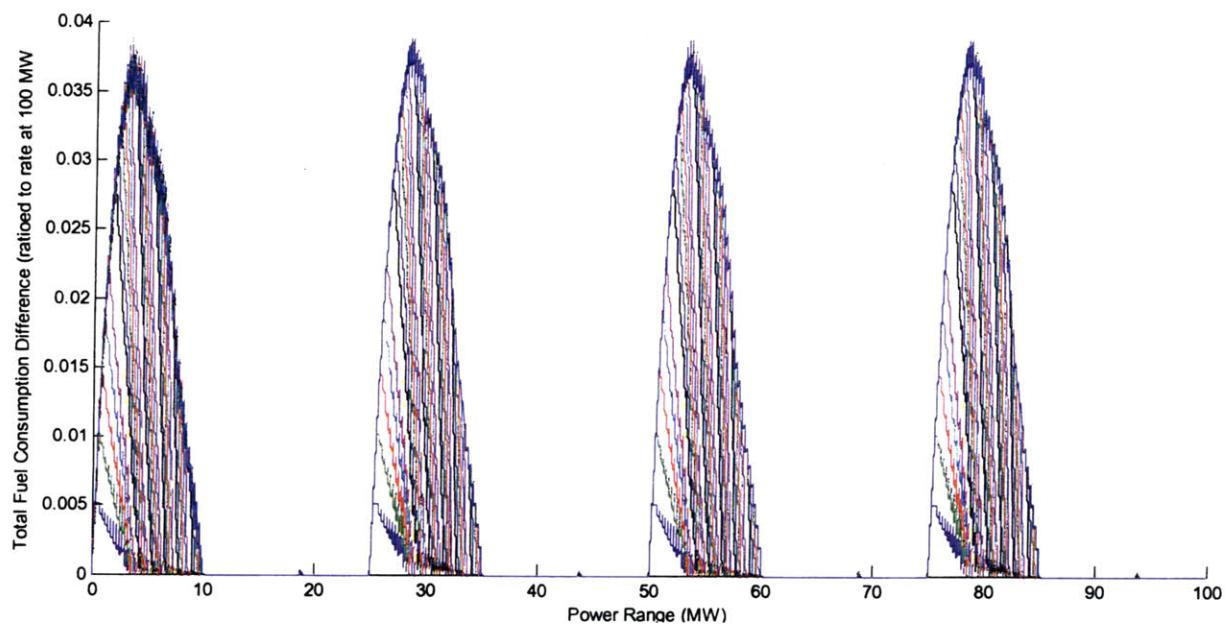
Figure 17: Fuel Consumption Difference Family of Curves

The final output from the optimization model is produced when the general fuel consumption curves as a function of power required are converted into total fuel consumed for a definite ship operating timeframe. This is accomplished within the optimization model by taking the family of total fuel consumption curves and considering the power required for each speed as well as the probability that the ship operates at that speed. The result is displayed in Figure 18 as a function of the number of installed fuel cells.
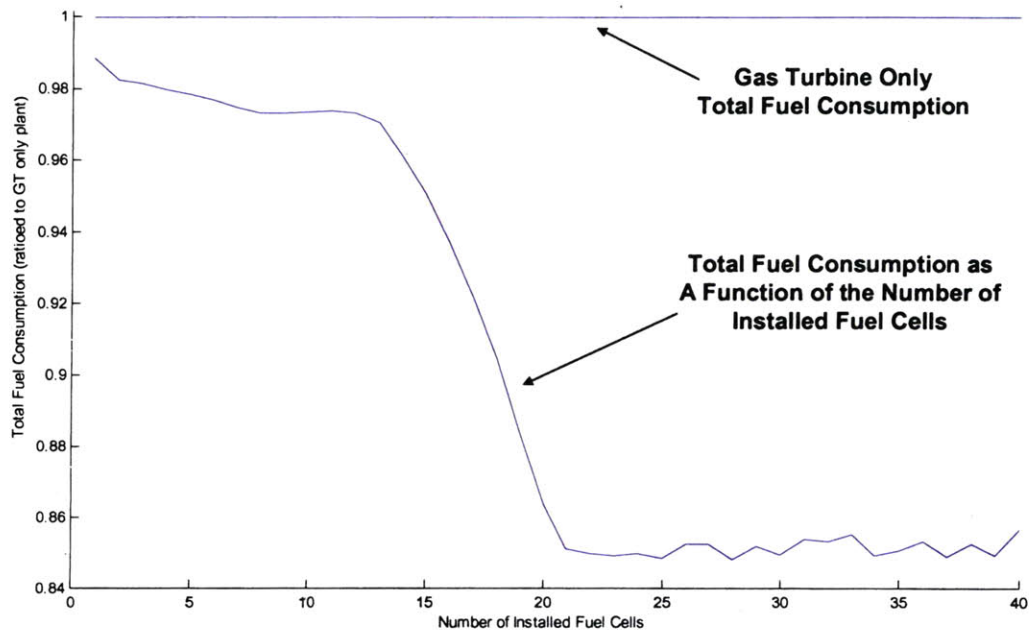
Figure 18: Total Fuel Consumption for a DDG-51 Speed Profile

These results show that there is little decrease in fuel consumption, on the order of 3%, until around 12 fuel cells or 3 MW of capacity, have been installed. At this point, total fuel consumption decreases rapidly for each additional fuel cell installed until a 20 bank fuel cell, totaling 5 MW of capacity, has been reached. At this point, the propulsion plant has experienced a 14% decrease in fuel consumption. Increasing the number of fuel cells past this point however does not continue lowering fuel consumption.

An ancillary program output is the operating status of the fuel cell bank required to achieve the optimal

fuel consumption at each required power. The fuel cell operating status for the 4 propulsion plant

configurations with 5, 10, 15, and 20 fuel cells for up to 10 MW is displayed in Figure 19.
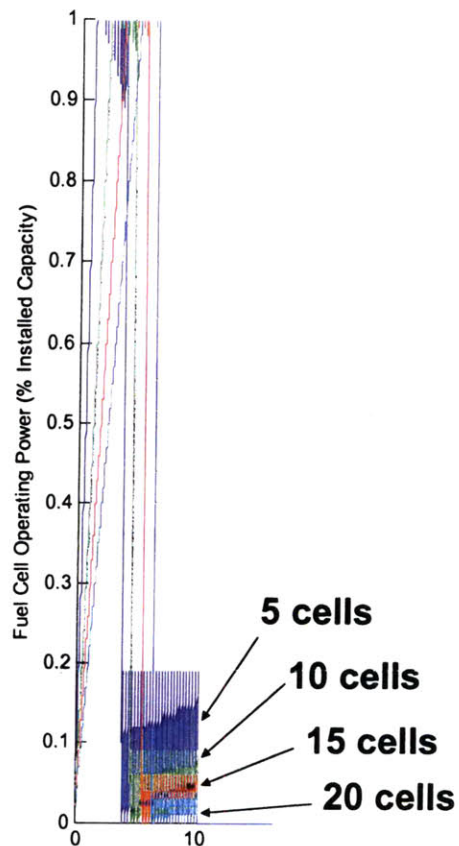
Figure 19: Fuel Cell Operating Scheme up to 10 MW

The gas turbine startup cycles are again seen to drive the desired fuel cell operation as 4 similar

operating patterns are observed at each of the regions where gas turbines hold a low partial load, seen

for a 100 MW range in Figure 20. Operation of the fuel cells from configuration to configuration is seen

to be similarly timed. All four plant configurations are seen to pick up the entire initial propulsion load

and operate fully loaded until about 5 MW of additional power is required. At this point each plant

begins shifting over to a partially loaded gas turbine. When the 10 MW partial load value has been

43

reached, the gas turbine is now operating efficiently enough to accept the entire load and all 4 fuel cell

banks are turned off.
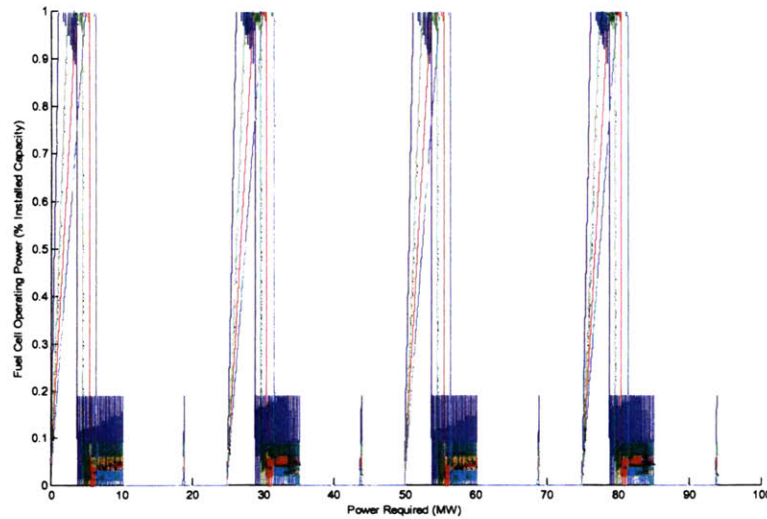
Figure 20: Fuel Cell Operating Scheme up to 100 MW

Finally, Table 4 is produced which shows for the 20 fuel cell configuration how best to operate each

piece of propulsion plant machinery.

Speed	Power	20 Fuel Cells	#1 GT	#2 GT	#3 GT	#4 GT
5	0.5 MW	10%	0%	0%	0%	0%
10	1.6 MW	32%	0%	0%	0%	0%
15	5.2 MW	100%	0.8%	0%	0%	0%
20	12.0 MW	0%	48%	0%	0%	0%
25	27.0 MW	40%	100%	0%	0%	0%
30	66.5 MW	0%	100%	100%	66%	0%
35	100.0 MW	0%	100%	100%	100%	100%

Table 4: Operating Scheme for a 20 Fuel Cell Propulsion Plant

An important item in this table is that for the first 3 speeds, the power required can be generated

almost solely by the fuel cell bank. Although this requires meticulous fuel and reactant gas flow control,

44

because the power levels are discrete, an automatic flow control system for quickly reaching the required output level can be used. The system would then require slight feedback control for fine tuning the power required during a several minute transient response. Another item of note is that for all speeds less than 25 knots, the fuel cells and a single gas turbine are sufficient for meeting any power demand.

4.2   Sensitivity Analysis

Now that the optimization model has been coded and simulations run, it is important to investigate some of the initial assumptions. The goal of this chapter is to increase the confidence in the models outcome by altering 2 variables and determining their significance on the final results. Sensitivity analysis in this manner also develops a focus for making recommendations on future areas of study.

4.2.1   Varying the Speed Profile

The first area looked at more in depth is with respect to the speed profile. Because four speed profile values fall within a gas turbine startup cycle region it was readily expected that fuel savings could be attained. Knowing how significant an impact the given speed profile on the savings in total fuel consumption will be found by shifting the probabilities from four speeds which fall within gas turbine inefficiency regions to those which can already be achieved in an efficient manner. This will be accomplished by decrementing the probability of operating at inefficient speeds while increasing the time spent at more fuel efficient speeds. Figure 21 represents the speed profiles used to conduct this analysis.
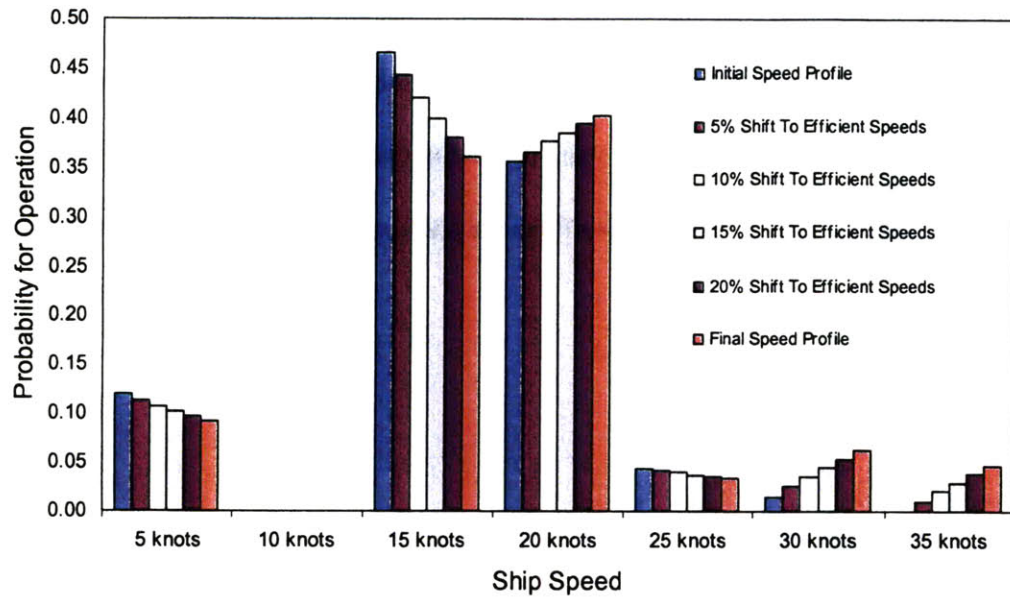
Figure 21: Decreasing Operation at All Inefficient Speeds

The resulting total fuel consumption seen in Figure 22 is highly sensitive to the speed profile. By shifting the speed probabilities by only 5%, the entire gain of 14% fuel savings originally possible by the 20 fuel cell installation is significantly impacted. As the speed profile is further shifted, the savings continue diminishing.
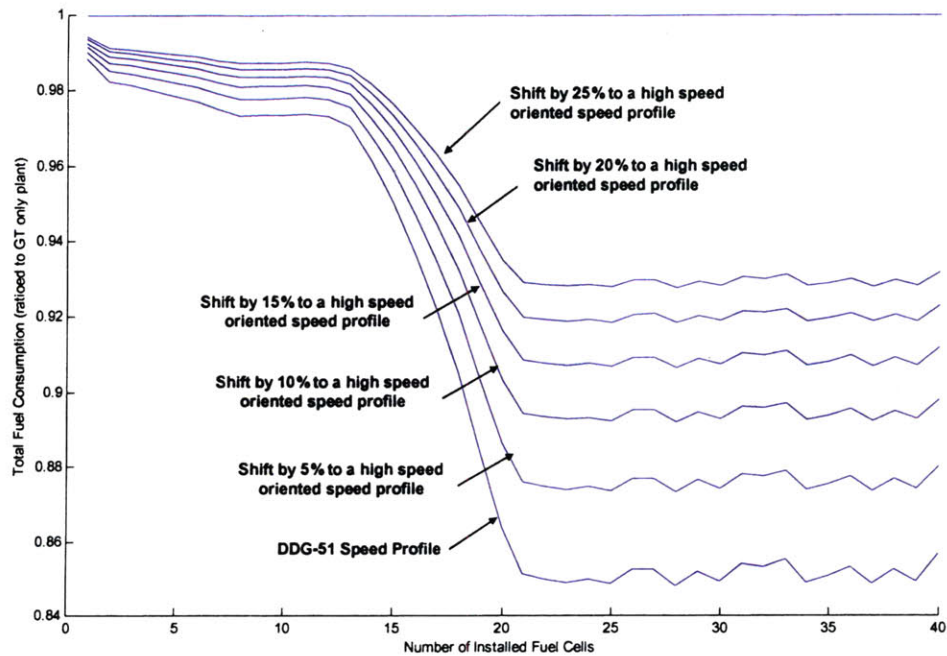
Figure 22: Steaming Profile Sensitivity Analysis for all Low Speeds

The next way to analyze the sensitive which speed has on total fuel consumption is to shift the speed

profile away from a single speed and toward the 3 speeds not affected by the gas turbine startup cycles.

This was accomplished by performing 5 runs which removed 10% of the time spent steaming at 15 knots

and replacing it by an equally distributed probability at higher speeds, shown in Figure 23.

47
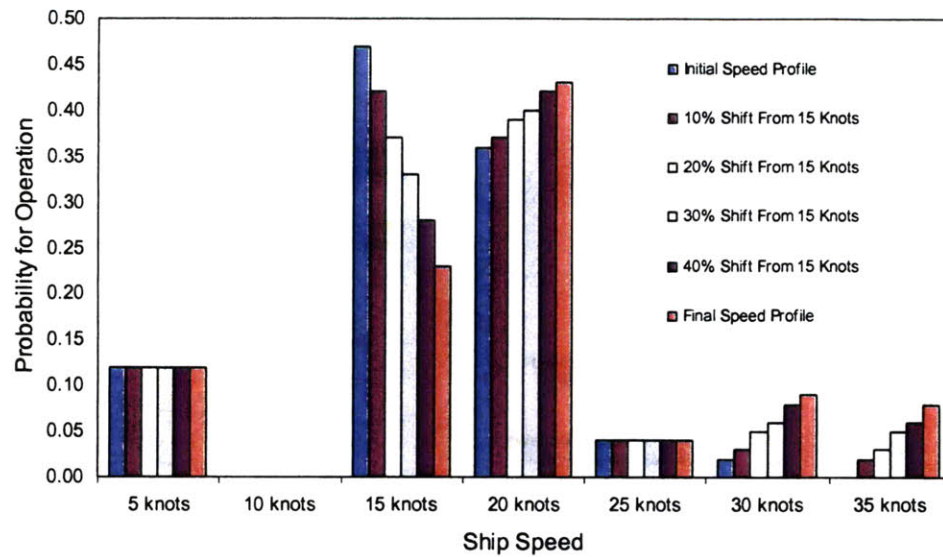
Figure 23: Decreasing Operation at a Single Inefficient Speed

The results of this analysis, displayed in Figure 24, show that again the makeup of the speed profile has a very significant impact on the resulting total fuel consumption. The opportunity for fuel cells to be effective in developing savings therefore is highly dependent on any changes the US Navy implements in how they operate this class of destroyer.
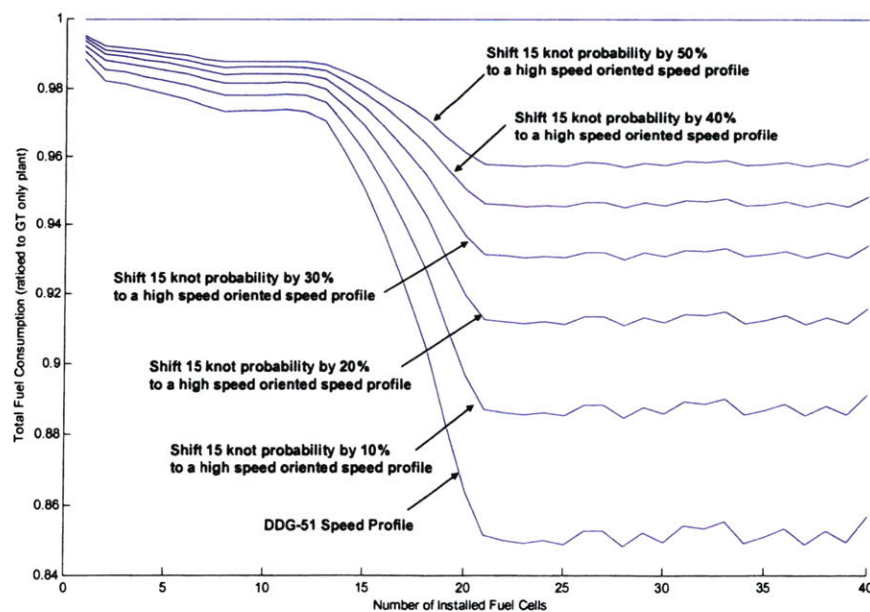
Figure 24: Steaming Profile Sensitivity Analysis Shifting Away from the 15 Knot Speed

48

In summary, slight modifications to the speed profile can drastically affect the resultant total fuel consumption. Installing fuel cells is beneficial to reducing fuel consumption but changes in the operational profile can cause drastic changes to this overall reduction, shown in Table 5.

Sensitivity Analysis	Modifying All Speeds	Modifying 15 Knots
Initial Speed Profile	14% Savings	14% Savings
1st Iteration	12% Savings	11% Savings
2nd Iteration	10% Savings	9% Savings
3rd Iteration	9% Savings	7% Savings
4th Iteration	8% Savings	5% Savings
Final Speed Profile	8.5% Savings	4% Savings

Table 5: Summary of Speed Profile Sensitivity Analysis

4.2.2 Varying PEMFC efficiency

The second area sensitivity analysis is warranted is with respect to the specific fuel consumption of the fuel cell. Although a 275 gram per kilowatt-hour quantity was assumed, because research in this area is ongoing in concert with the automobile industry, advances may be made. This has to potential for making the fuel cell more efficient. Conversely, if a valid hydrogen infrastructure is not enacted in the near future, and onboard reforming of traditional engine fuels proves more challenging than currently expected, this value may be much lower. Accordingly, total fuel consumption as a function of installed fuel cell capacity was determined for fuel cell specific fuel consumptions in 5% increments as shown in Figure 25.
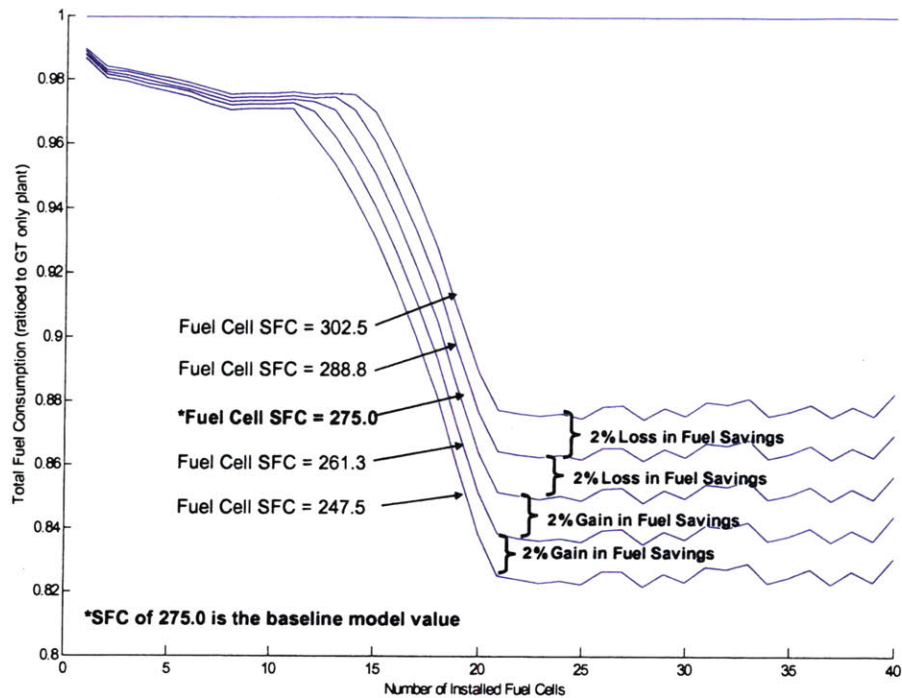
Figure 25: Consumption Sensitivity based on Fuel Cell SFC

Compared to the results of the speed profile sensitivity analysis, total fuel consumption appears relatively stable when exposed to changes in the fuel cells specific fuel consumption. For each of the 5% SFC increments, increasing or decreasing, the fuel consumption curves exhibit an extremely tight shape and show little deviation with a low number of fuel cells installed. As the number of fuel cells increases, there is a 2% deviation in total fuel savings for each increment, but the overall shape remains intact and is therefore predictable.

5.   Hybrid Propulsion Plant Integration

The results of the propulsion plant optimization program in chapter 4 have shown that installing 5 MW of PEM fuel cells have the potential for providing up to a 14% decrease in fuel consumption for the DDG-51 Flight 1 hull under a reasonable steaming profile. This chapter discusses the naval architecture

ramifications of installing such a system shipboard by using the ship modeling tool ASSET® version 5.3 which is capable of comparing a hybrid propulsion plant ship to one that is gas turbine only driven.

The benefit of fuel cell use aboard US naval surface combatants is seen because they increase the overall fuel efficiency of propulsion equipment while operating at desired speeds. This benefit directly translates into less fuel used during a transit, or to an overall longer deployment as the ship now possesses increased endurance. Either of these options translates into less money being spent.

These savings can also be manifest in a more indirect manner. If the hybrid fuel cell and gas turbine propulsion plant is implemented at the early concept design phase, fuel tanks can be sized appropriately for the given mission, and a more optimized design can be developed.

Early stage design of the hybrid propulsion plant would also allow for the fuel cells and supporting equipment to be arranged in an efficient manner. Characteristics such as survivability, maintainability, manufacturability, and operational considerations could also be designed for in this scenario. ASSET® is first used to analyze the gas turbine only ship, with the machinery arrangement of the DDG-51 shown in Figure 26.

AP   FP

1.0   0.9   0.8   0.7   0.6   0.5   0.4   0.3   0.2   0.1   0.0

                              SCALE

                0   20   40   60 M
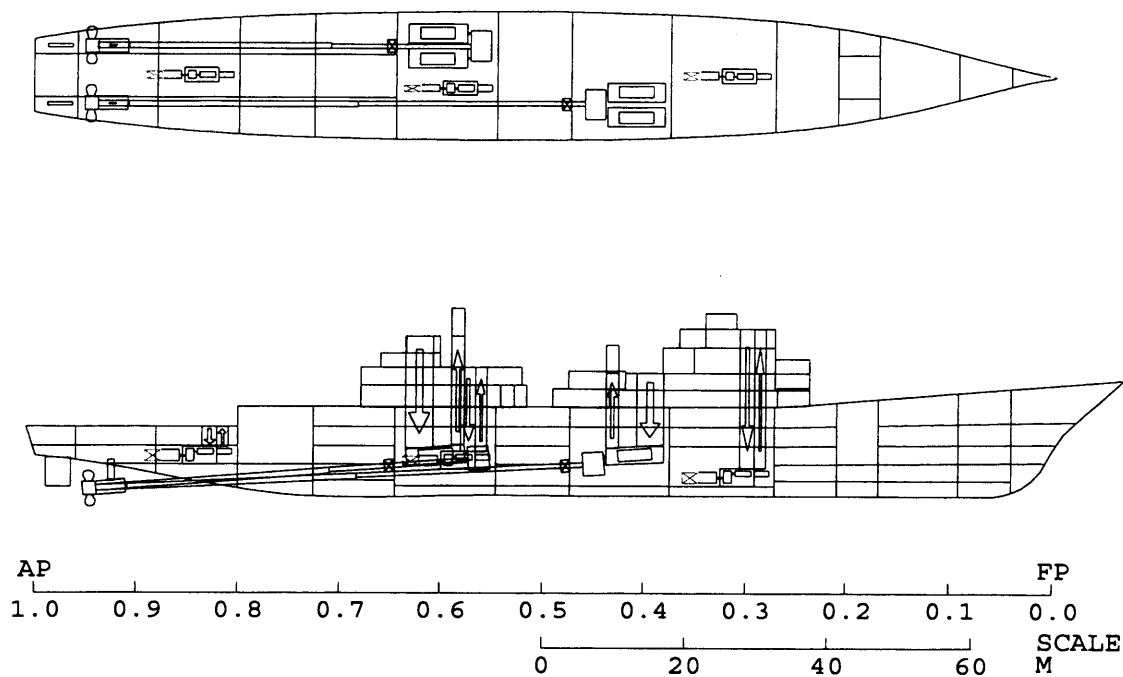
Figure 26: DDG-51 Machinery Layout

In this study, fuel cell use can lead to 14% of the fuel tanks not being required to achieve the requisite 4000 nautical miles currently experienced by destroyers. DDG-51 designs dedicate 2,000 m^3 of the ship's total 28,000 m^3 in hull volume to fluid storage tanks. Of this amount, 1,522 m^3, or just over 75%, is used for storing the ships 1,145 metric tons of fuel. By decreasing this amount by 160 metric tons, sufficient space becomes available to house the fuel cells and any additional hybrid plant machinery, including power generation, mechanical transmission, and chemical support components. The DDG-51 hull form primary characteristics are shown in Table 6.

```
        PRINCIPAL CHARACTERISTICS - M              WEIGHT SUMMARY - MTON
    LBP                           142.0      GROUP 1 - HULL STRUCTURE   3275.5
    HULL LOA                      153.4      GROUP 2 - PROP PLANT        761.3
    BEAM, DWL                      18.0      GROUP 3 - ELECT PLANT       317.6
    DEPTH @ STA 10                 12.7      GROUP 4 - COMM + SURVEIL    436.1
    DRAFT TO KEEL DWL               6.2      GROUP 5 - AUX SYSTEMS       856.7
    DRAFT TO KEEL LWL               6.7      GROUP 6 - OUTFIT + FURN     663.0
    FREEBOARD @ STA 3               7.4      GROUP 7 - ARMAMENT          320.0
    GMT                             0.9      -----------------------------------
    CP                            0.587      SUM GROUPS 1-7             6630.3
    CX                            0.825      DESIGN MARGIN               829.6
                                             -----------------------------------
                                             LIGHTSHIP WEIGHT           7459.9
    SPEED(KT):   MAX= 30.5  SUST= 29.3       LOADS                      1710.4
    ENDURANCE:  3697.0 NM AT 20.0 KTS        -----------------------------------
                                             FULL LOAD DISPLACEMENT     9170.3
    TRANSMISSION TYPE:       MECH            FULL LOAD KG:  M              7.8
    MAIN ENG: 4 GT       @ 19220.4 KW
                                             MILITARY PAYLOAD WT- MTON  1115.8
    SHAFT POWER/SHAFT:     37487.0 KW        USABLE FUEL WT - MTON      1145.5
    PROPULSORS: 2 - CP        - 5.2 M DIA

    SEP GEN:  3 GT       @  2500.0 KW
                                                  OFF   CPO   ENL   TOTAL
    24-HR LOAD                   2377.1      MANNING   26    24   291    341
    MAX MARG ELECT LOAD          3600.8      ACCOM     29    27   321    377

        REQUIRED AREA SUMMARY - M2               AVAILABLE AREA SUMMARY - M2
    OTHER AREA            -      5180.        HULL AREA          -       3995.
    SUPERSTRUCTURE AREA   -      1161.        SUPERSTRUCTURE AREA   -    1896.
    ----------------------------------        ----------------------------------
    TOTAL AREA           -       6341.        TOTAL AREA         -       5891.

        REQUIRED VOLUME SUMMARY - M3             AVAILABLE VOLUME SUMMARY - M3
    OTHER VOLUME         -      25072.        HULL VOLUME        -      22126.
    SUPERSTRUCTURE VOLUME -     2920.         SUPERSTRUCTURE VOLUME -    5403.
    ----------------------------------        ----------------------------------
    TOTAL VOLUME         -      27992.        TOTAL VOLUME       -      27529.
```

Table 6: ASSET® 5.3 DDG-51 Design Summary

To adapt the surface combatant hull, several modifications were made to the original DDG-51 model to allow for a hybrid propulsion plant. The first was that usable fuel weight was decreased by 14% to 985 metric tons. The design tool uses this parameter to develop all tanks, which it then places inside the hull. The locations of these tanks directly affect the placement of compartment subdivisions. By affecting the locations of transverse bulkheads, and other structural components, this step in the process plays a large role in determining the ship's large scale naval architecture parameters such as displacement, draft, and operating performance. In this case it is expected that the lower required fluid

volume will translate into slightly smaller ship, but because the fuel cells and supporting components
are heavier, the ship will have a slightly larger draft and sit lower in the water.

The next step to investigating a hybrid propulsion plant model for a surface combatant was modifying
the machinery room spaces and layout. The ship's service generator located in the forward most
auxiliary machinery room was shifted aft to provide deck space for the fuel cells. To emulate the effect
that 5 MW of fuel cells and supporting equipment, including onboard fuel reformation, would have on
the ship's architecture, a weight and space adjustment was made to the ships requirements table. Using
the integrated propulsion system worksheet provided by the Electric Ship Program Office, 5 MW of fuel
cells can reasonably be expected to require a 7 x 4.3 meter surface area profile and weigh 77 metric
tons. Several support system items were also installed in this manner, which are summarized in Table 7.

Removed from Ship	Weight	Area	Volume	Length	Width	Height
14% of Fuel Tank Capacity	160 MT	140 m^2	210 m^3	From Various Locations		
Components Added	Weight	Area	Volume	Length	Width	Height
5.0 MW PEM Fuel Cell	77 MT	30.1 m^2	148 m^3	7.0 m	4.3 m	4.9 m
Onboard Reforming Plant	65 MT	18.5 m^2	46.2 m^3	4.2 m	4.4 m	2.5 m
Chemical Support System	8.4 MT	7.8 m^2	13.2 m^3	3.4m	2.3m	1.7m
Mechanical Support Systems	54 MT	15.0 m^2	5.0 m^3	Group of Multiple Components		
Electrical Support Systems	32 MT	9.4 m^2	3.1 m^3	Group of Multiple Components		
Total Added	236.4 MT	80.8 m^2	215.5 m^3			

Table 7: Ship and Equipment Modifications

Once the adjustments to the fuel tanks and machinery rooms were made within the model data base,
the final step was to have ASSET® compile and synthesize the hybrid ship. To ensure ease of operation,

54

the hybrid plant machinery layout is seen to be very similar to the DDG-51 flight 1 layout and is shown in

Figure 27.
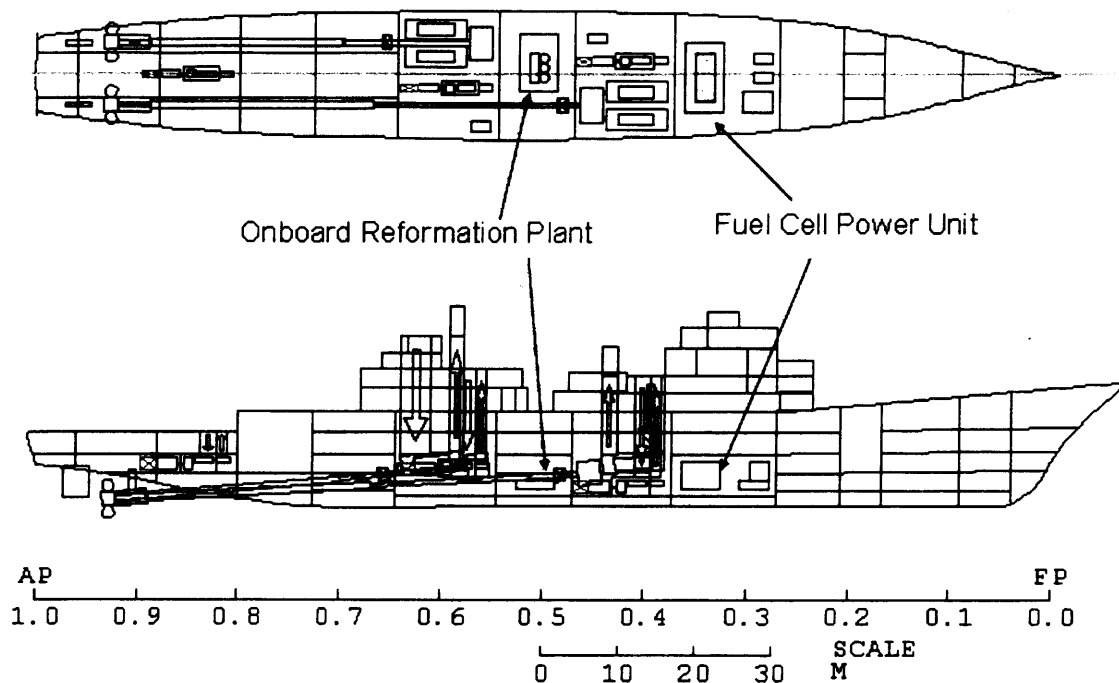
Figure 27: Hybrid Propulsion Plant

Although the machinery layout doesn't reveal significant structural changes to the ship's architecture, there are notable changes to the overall geometry and principle characteristics, shown in Table 8. The ship has become significantly smaller, displacing 250 metric tons less than the DDG-51 hull. Both length and beam have also decreased, to 134.0 meters and 16.9 meters respectively. Also of note is that the ships center of gravity has moved to lower in the ship by almost a full meter. This shows that fuel tanks were likely taken from relatively high in the ship while the more mass dense electric and mechanical components to be installed were placed low. Additionally, this new center of gravity has served to raise the ships meta-centric height from 0.9 meters to 1.2 meters, which means that the ship will exhibit a higher initial static stability.

```
        PRINCIPAL CHARACTERISTICS - M              WEIGHT SUMMARY - MTON
LBP                            134.0      GROUP 1 - HULL STRUCTURE   3014.7
HULL LOA                       144.7      GROUP 2 - PROP PLANT       1052.8
BEAM, DWL                       16.9      GROUP 3 - ELECT PLANT       302.5
DEPTH @ STA 10                  12.7      GROUP 4 - COMM + SURVEIL    426.9
DRAFT TO KEEL DWL                6.2      GROUP 5 - AUX SYSTEMS       807.2
DRAFT TO KEEL LWL                7.1      GROUP 6 - OUTFIT + FURN     633.5
FREEBOARD @ STA 3                7.0      GROUP 7 - ARMAMENT          319.9
GMT                              1.2      -------------------------------
CP                             0.587      SUM GROUPS 1-7             6557.4
CX                             0.825      DESIGN MARGIN              820.5
                                          -------------------------------
                                          LIGHTSHIP WEIGHT          7377.9
SPEED(KT):   MAX= 30.0  SUST= 28.7        LOADS                     1541.5
ENDURANCE:  3094.1 NM AT 20.0 KTS         -------------------------------
                                          FULL LOAD DISPLACEMENT    8919.4
TRANSMISSION TYPE:        MECH            FULL LOAD KG:  M             6.9
MAIN ENG: 4 GT      @ 19220.4 KW
                                          MILITARY PAYLOAD WT- MTON 1115.8
SHAFT POWER/SHAFT:    37487.0 KW          USABLE FUEL WT - MTON      985.0
PROPULSORS: 2 - CP      - 5.2 M DIA

SEP GEN:  3 GT      @  2500.0 KW
                                               OFF   CPO   ENL   TOTAL
24-HR LOAD                    2265.6      MANNING  26    24    291    341
MAX MARG ELECT LOAD           3382.8      ACCOM    29    27    321    377

      REQUIRED AREA SUMMARY - M2             AVAILABLE AREA SUMMARY - M2
OTHER AREA            -      5376.      HULL AREA            -      3674.
SUPERSTRUCTURE AREA  -      1104.      SUPERSTRUCTURE AREA  -      1599.
-----------------------------------   -----------------------------------
TOTAL AREA           -      6480.      TOTAL AREA           -      5273.

      REQUIRED VOLUME SUMMARY - M3            AVAILABLE VOLUME SUMMARY - M3
OTHER VOLUME          -     24755.      HULL VOLUME          -     19562.
SUPERSTRUCTURE VOLUME -      2776.      SUPERSTRUCTURE VOLUME -      4566.
-----------------------------------   -----------------------------------
TOTAL VOLUME         -     27531.      TOTAL VOLUME         -     24128.
```

Table 8: Hybrid Ship Principle Characteristics

A side by side comparison of the ship's key characteristics is in Table 9. This table shows that even though fuel cells with all of their support systems considered are larger per megawatt of power delivered than gas turbines, because they create a large enough fuel savings, their installation can potentially serve to make the ship smaller and more stable.

Hull	DDG-51 Flight 1	Hybrid Surface Combatant	Difference (% of Reference Value)
Displacement	9,170 metric tonns	8,919 metric tonns	2.7% Reduction
Length	144.7 meters	134.0 meters	7.4% Reduction
Beam	18.0 meters	16.9 meters	6.1% Reduction

Draft	6.7 meters	7.1 meters	6.0% Increase
Meta-centric Height	0.9 meters	1.2 meters	33.3% Increase
KG	7.8 meters	6.9 meters	11.5% Reduction

Table 9: Principle Characteristics Comparison Table

6. Summary

Fuel cells are a nontraditional power source and create electricity in a clean and efficient manner. Although there are many types being researched and in operation in the commercial sector, PEMFCs present promise for use onboard US naval ships over the next 20 years. That being said, there are many technical hurdles yet to be overcome in the commercial realm before PEMFC's possess the robustness and power density to serve this function.

In summary, 5 MW of fuel cells when installed onboard the current DDG-51 hull form produce a 14% fuel savings. Although an optimization model has shown this fuel savings in Chapter 4, and a ship modeling tool has displayed rough order technical feasibility in Chapter 5, there are substantial difficulties when attempting to install a nontraditional power source onboard an already designed destroyer. These include having to conduct detailed design within the machinery room and evaluate the ship's fuel tank layout to ensure the changes do not impede operation and maintainability. Additionally, the effects on ships performance will also have to be reexamined as there are changes to the ship's center of gravity.

If installing 5MW of fuel cells onboard the DDG-51 hull form is not possible, placing them in a gas turbine propulsion plant on another hull form is also beneficial, but again presents challenges. Although the fuel savings results could be similar, the selected hull's resistance curve would have to be investigated to identify which speeds are in fact the most fuel inefficient and compare those results in

light of that hulls speed profile. A different hull form with a new operational profile may mitigate some of the results shown in this research on the DDG-51 hull.

Finally, if fuel cells cannot be installed onboard the current DDG-51 or any future gas turbine only surface ships, the operating status quo should be modified in an attempt to save fuel within the constraints of already existing machinery layouts. There are two ways this can be accomplished. The first is by operating gas turbines in series wherever possible. For a given engine order, this method will force more fuel efficient gas turbine operation. The second is by favoring speeds which keep all operating gas turbines as highly loaded as possible. The ship's resistance curve should be carefully analyzed and speeds avoided as much as possible which force a gas turbine to be loaded with less than 10 MW of power.

7. Bibliography

O'Hayre, R. Cha, S.W, Colella, W., Prinz, F. B. (2009). *Fuel Cell Fundamentals.* John Wiley & Sons, New York.

Spiegel, C. (2008). *PEM Fuel Cell Modeling and Simulation Using MATLAB®.* Academic Press, London.

Woud, H. C., Stapersma, D. (2002). *Design of Propulsion and Electric Power Generation Systems.* IMarEST Publications, London.

Appendix: Propulsion Plant Model Code

The model developed from the algorithm described in chapter 3 is here listed as MATLAB® code. Results

of the code in the form of output tables are found in chapter 4 of the main text.

```
close all;
clear all;
hold on;

grams_to_lbs=0.0022046224760379584;
lbs_to_LT=0.00044642857;

Electric_required = (1:10:100000);

%Input Power Source Details:

%Currently Installed Gas Turbines:
GT_available = 4; %Establish number of installed Gas Turbines
GT_sfc = [750 750 730 710 690 670 650 630 610 590 575 555 535 512 495 480 464 442 432 420 409 400
391 382 372 361 352 342 331 322 316.5 311 305.5 300 296 292 288 284 280 276 272 268 265 262 259
257 255 253 251 250 249 248 247 246 245 244 243.25 242.7 242.5 241.8 241.25 240.6 240 239.5 239
238.85 238.75 238.25 238 237.75 237.5 237.25 237 235.75 236.25 235.85 235.6 235.3 235 234.75
234.25 233.85];
GT_power_range = 25000;  %Establish relationship from kw power to GT Specific Fuel Consumption
Array in g/kw*h
GT_installed = GT_available * GT_power_range; %GT kw installed/available
plot(GT_power_range/(1000*length(GT_sfc)):GT_power_range/(1000*length(GT_sfc)):GT_power_range/100
0,GT_sfc)
xlabel('Power Range (MW)')
ylabel('Specific Fuel Consumption (grams per kwh)')

%Potentially Available Fuel Cells:
FC_linear_sfc = 247.5;   %CONSERVATIVE FC sfc EFFICIENCY..
FC_available = 4; %Number of fuel cells installed
FC_sfc = [FC_linear_sfc FC_linear_sfc];   %Establish FC Specific Fuel Consumption Array
FC_power_range = 1250;
%plot(0:FC_power_range/length(FC_sfc)+1:FC_power_range,FC_sfc)

for n=1:FC_available

FC_installed = n * FC_power_range; %Assign FC kw installed/available for test

Installed_power=GT_installed+FC_installed;

        %if GT_installed<Electric_required(length(Electric_required)) %confirm GT alone can power
ship
        %    display ('not enough GT installed power');
        %end

        %if Installed_power<Electric_required(length(Electric_required)) %confirm configuration
provides enough power
        %    display ('not enough total installed power');
        %end

        FC_active=1;

for l=1:length(Electric_required)   %increment through each element of the electric required
domain
    %Best_use_ratio(l)=0
    %BLOCK 1 - Find most efficient operating conditions for given installed power

    GTs_required=fix(Electric_required(l)/GT_power_range);
    Nominal_GT_load=Electric_required(l)-GTs_required*GT_power_range;
    GT_partial_efficiency=fix(100*Nominal_GT_load/GT_power_range);
```

```
        if GT_partial_efficiency<=1
            GT_partial_efficiency=1;
        end

        if GT_partial_efficiency>=length(GT_sfc)
            GT_partial_efficiency=length(GT_sfc);
        end

        Nominal_GT_efficiency=GT_sfc(GT_partial_efficiency);

        %GT_parallel_efficiency_two=GT_sfc(1+fix(GT_partial_efficiency/2));
        %if GT_parallel_efficiency_two<=1
        %    GT_parallel_efficiency_two=1;
        %end


GT_parallel_efficiency_all=fix(length(GT_sfc)*Electric_required(1)/Electric_required(length(Elect
ric_required)));

        if GT_parallel_efficiency_all<=1
            GT_parallel_efficiency_all=1;
        end

        if GT_parallel_efficiency_all>=length(GT_sfc)
            GT_parallel_efficiency_all=length(GT_sfc);
        end

        Nominal_GT_parallel_efficiency_all=GT_sfc(GT_parallel_efficiency_all);


Fuel_consumption(1,n)=GTs_required*GT_power_range*GT_sfc(length(GT_sfc))+Nominal_GT_load*Nominal_
GT_efficiency;
        GT_only_consumption(1,n)=Fuel_consumption(1,n); %tabulate GT only fuel consumption at all
powers - BASELINE


%GT_parallel_consumption_two(1,n)=(GTs_required*GT_power_range+Nominal_GT_load)*GT_parallel_effic
iency_two;
        GT_parallel_consumption_all(1,n)=Electric_required(1)*Nominal_GT_parallel_efficiency_all;



        %Find Combined fuel consumption and compare it to GT only value:

        for m=FC_active:100; %increment loading of installed power to include fraction(m/100) of
FC

        if m*FC_installed/100<=Electric_required(1)   %only increment FC loading if needed

            FC_loading(m)=m*FC_installed/100; %Load n installed FCs to m fraction of loading
            GT_loading(m)=Electric_required(1)-FC_loading(m);   %Power remaining to be supplied
with GTs

        if GT_loading(m)<=0 %set zero GT load if FC powering is sufficient
            GT_loading(m)=0;
        end

    %Assume GTs are brought online in series (ie MOST effeciently)
    %Find partially loaded GT Efficiency:
    GTs_fully_loaded=fix(GT_loading(m)/GT_power_range);
    Partial_GT_load(m)=GT_loading(m)-GTs_fully_loaded*GT_power_range;

    GT_operation(m)=fix(100*Partial_GT_load(m)/GT_power_range);


        if GT_operation(m)<=1
            GT_operation(m)=1;
        end

        if GT_operation(m)>=length(GT_sfc)
            GT_operation(m)=length(GT_sfc);
```

61

```matlab
        end

    FC_operation(m)=fix(100*FC_loading(m)/(n*FC_power_range));

    if FC_operation(m)==0
        FC_operation(m)=1;
    end

    if FC_operation(m)>=length(FC_sfc)
        FC_operation(m)=length(FC_sfc);
    end

    FC_efficiency(m)=FC_sfc(FC_operation(m));
    GT_efficiency(m)=GT_sfc(GT_operation(m));

        %Find Combined fuel consumption and compare it to GT only value:

Potential_fuel_consumption(1,n)=FC_loading(m)*FC_efficiency(m)+GTs_fully_loaded*GT_power_range*GT
_sfc(length(GT_sfc))+Partial_GT_load(m)*GT_efficiency(m);

        if Fuel_consumption(1,n)>=Potential_fuel_consumption(1,n)
            Fuel_consumption(1,n)=Potential_fuel_consumption(1,n);
            Best_use_ratio(1,n)=m/100;

        end
        end
    end

    Fuel_consumption_differential(1,n)=GT_only_consumption(1,n)-Fuel_consumption(1,n);

end

    Cumulative_fuel_consumption(1,n)=Fuel_consumption_differential(1,n); %establish fixed point
to integrate from

    for a=2:(length(Electric_required)-1)
        Cumulative_fuel_consumption(a,n)=Cumulative_fuel_consumption(a-
1,n)+Fuel_consumption_differential(a-1,n);
    end


Cumulative_fuel_consumption(length(Electric_required),n)=Cumulative_fuel_consumption(length(Elect
ric_required)-1,n)+Fuel_consumption_differential(length(Electric_required),n);

end

%GT_only_consumption=GT_only_consumption*grams_to_lbs*lbs_to_LT;
%Fuel_consumption=Fuel_consumption*grams_to_lbs*lbs_to_LT;
%LT_Fuel_per_10000NM=sum(GT_only_consumption)-sum(Fuel_consumption);

%Input Ship Profile Data:
Power_array = [5 10 15 20 25 30 35];   % Establish knots Power conversion Array (in 5 knot
increments)
Power_required = [500 1600 5200 12000 27000 66500 100000];   %KW resistance to overcome
Endurance = 4000; %Nautical miles endurance
Speed_profile = [.119 0 .466 .356 .044 .015 0]; %Profile from ASSET 5.3 Flight 1 Mission Analysis
Module

%Speed_profile = [.11305 0 .4427    .366483333  .0418   .025483333  .010483333];
%Speed_profile = [.1073975 0 .420565 .3764425 .03971 .0354425 .0204425];
%Speed_profile = [.102027625 0 .39953675 .385903708 .0377245 .044903708 .029903708];
%Speed_profile = [.096926244    0 .379559913 .394891856 .035838275 .053891856 .038891856];
%Speed_profile = [.092079932 0 .360581917 .403430597 .034046361 .062430597 .047430597];

%Speed_profile = [0.119 0    0.4194  0.371533333 0.044    0.030533333 0.015533333];
%Speed_profile = [0.119 0    0.3728  0.387066667 0.044    0.046066667 0.031066667];
%Speed_profile = [0.119 0    0.3262  0.4026  0.044   0.0616  0.0466];
%Speed_profile = [0.119 0    0.2796  0.418133333 0.044    0.077133333 0.062133333];
%Speed_profile = [0.119 0    0.233   0.433666667 0.044    0.092666667 0.077666667];

%Speed_profile = [1/7 1/7 1/7 1/7 1/7 1/7 1/7]; %Average use distribution
```

```matlab
%Speed_profile = [.025 .075 .2 .4 .2 .075 .025]; %Normal Distribution
%Speed_profile = [.025 .025 .05 .1 .2 .25 .35]; %High speed ops
%Speed_profile = [.35 .25 .2 .1 .05 .025 .025]; %Low speed ops
%Speed_profile = [0 0 0 0 1 0 0]; %Test profile
%Speed_profile = [1/5 1/5 1/5 0 1/5 0 1/5]; %No pickup effect
%Speed_profile = [1/3 1/3 0 0 1/3 0 0]; %least preferred profile (high argument for fuel cells
%Speed_profile = [0 0 0 1/3 0 1/3 1/3]; %optimal GT profile

%Speed_profile = [1 0 0 0 0 0 0]; %5 knots dominant
%Speed_profile = [0 1 0 0 0 0 0]; %10 knots dominant
%Speed_profile = [0 0 1 0 0 0 0]; %15 knots dominant
%Speed_profile = [0 0 0 1 0 0 0]; %20 knots dominant
%Speed_profile = [0 0 0 0 1 0 0]; %25 knots dominant
%Speed_profile = [0 0 0 0 0 1 0]; %30 knots dominant
%Speed_profile = [0 0 0 0 0 0 1]; %35 knots dominant


normalize3=GT_parallel_consumption_all(length(GT_parallel_consumption_all));
figure;
hold on;
plot(10*Electric_required/length(Electric_required),GT_only_consumption/normalize3)
%plot(Electric_required/length(Electric_required),GT_parallel_consumption_two/normalize3)
plot(10*Electric_required/length(Electric_required),GT_parallel_consumption_all/normalize3)
xlabel('Power Range (MW)')
ylabel('GT Fuel Consumption (Ratioed to 100 MW amount)')

figure;
hold on;
plot(10*Electric_required/length(Electric_required),(GT_parallel_consumption_all-
GT_only_consumption)/(normalize3))
xlabel('Power Range (MW)')
ylabel('Parallel to Series GT Operation Fuel Consumption Differential')



normalize2=GT_only_consumption(length(GT_only_consumption));
figure;
hold on;
plot(10*Electric_required/length(Electric_required),GT_only_consumption/normalize2)
plot(10*Electric_required/length(Electric_required),Fuel_consumption/normalize2)
xlabel('Power Range (MW)')
ylabel('Fuel Consumption (Ratioed to rate at 100 MW)')

figure;
hold on;
plot(Electric_required/10^3,Fuel_consumption_differential/(normalize2))
%plot(Electric_required,Cumulative_fuel_consumption/75)

figure;
hold on;
plot(Power_required/1000,Power_array)

figure;
hold on;
plot((1:length(Best_use_ratio))/100,Best_use_ratio);

if length(Power_array) ~= length(Speed_profile)  ;%confirm speeds used alligns with powers
available
    display ('Speed Profile is incorrect');
end

%Speeds_used = length(Speed_profile); %Set number of speeds in the profile
%Profile_check = sum(Speed_profile); %Verify profile is complete
%if Profile_check ~= 1.0000;
%    display ('Speed Profile is incorrect');
%end

%Total_fuel_saved_test(n)=0;
Total_fuel_saved(FC_available)=0;
Total_fuel_used_GT_only(FC_available)=0;
Total_fuel_used_hybrid(FC_available)=0;
```

```matlab
for n=1:FC_available

    for k=1:length(Speed_profile)


Power_for_speed(k)=fix(length(Electric_required)*Power_required(k)/Electric_required(length(Elect
ric_required)));

    if Power_for_speed(k)<=1
        Power_for_speed(k)=1;
    end

    if Power_for_speed(k)>=length(Electric_required)
        Power_for_speed(k)=length(Electric_required);
    end

    Fuel_used_GT_only(k,n)=Endurance*Speed_profile(k)*GT_only_consumption(Power_for_speed(k),n);
    Fuel_used_hybrid(k,n)=Endurance*Speed_profile(k)*Fuel_consumption(Power_for_speed(k),n);

Fuel_saved(k,n)=Endurance*Speed_profile(k)*Fuel_consumption_differential(Power_for_speed(k),n);

    Total_fuel_used_GT_only(n)=Total_fuel_used_GT_only(n)+Fuel_used_GT_only(k,n);
    Total_fuel_used_hybrid(n)=Total_fuel_used_hybrid(n)+Fuel_used_hybrid(k,n);
    Total_fuel_saved(n)=Total_fuel_saved(n)+Fuel_saved(k,n);

    %Total_fuel_saved_test(n)=Total_fuel_saved_test(n)+Fuel_used_GT_only(k,n)-
Fuel_used_hybrid(k,n);
    %Test=Total_fuel_saved(n)-Total_fuel_saved_test(n)

    end

end

%Total_fuel_used_GT_only(n)
%Total_fuel_used_hybrid(n)

%for n=1:FC_available
%    Total_fuel_saved(n)
%end

TFUplot1 = [0.9904    0.9854    0.9845    0.9832    0.9821    0.9808    0.9792    0.9777
0.9778    0.9779    0.9782    0.9777    0.9755    0.9679    0.9590    0.9476    0.9348    0.9208
0.9032    0.8865    0.8762    0.8750    0.8743    0.8750    0.8739    0.8772    0.8772    0.8735
0.8767    0.8745    0.8784    0.8777    0.8793    0.8743    0.8756    0.8776    0.8740    0.8771
0.8744    0.8805];
TFUplot2 = [0.9918    0.9875    0.9868    0.9857    0.9847    0.9837    0.9822    0.9810
0.9811    0.9811    0.9814    0.9810    0.9791    0.9727    0.9651    0.9554    0.9445    0.9325
0.9175    0.9033    0.8945    0.8936    0.8930    0.8935    0.8926    0.8954    0.8954    0.8922
0.8949    0.8931    0.8964    0.8959    0.8972    0.8929    0.8940    0.8958    0.8926    0.8953
0.8930    0.8982];
TFUplot3 = [0.9929    0.9892    0.9886    0.9876    0.9868    0.9859    0.9846    0.9835
0.9836    0.9837    0.9839    0.9836    0.9819    0.9764    0.9698    0.9614    0.9520    0.9416
0.9287    0.9164    0.9087    0.9079    0.9074    0.9079    0.9071    0.9095    0.9095    0.9068
0.9091    0.9075    0.9104    0.9099    0.9111    0.9074    0.9083    0.9098    0.9071    0.9095
0.9074    0.9120];
TFUplot4 = [0.9938    0.9906    0.9900    0.9892    0.9884    0.9876    0.9866    0.9856
0.9857    0.9857    0.9859    0.9856    0.9842    0.9793    0.9736    0.9662    0.9580    0.9489
0.9375    0.9268    0.9201    0.9194    0.9189    0.9194    0.9186    0.9207    0.9208    0.9184
0.9204    0.9190    0.9215    0.9211    0.9221    0.9189    0.9197    0.9210    0.9187    0.9207
0.9189    0.9229];
TFUplot5 = [0.9945    0.9916    0.9911    0.9904    0.9898    0.9891    0.9881    0.9873
0.9873    0.9874    0.9876    0.9873    0.9860    0.9817    0.9766    0.9701    0.9628    0.9548
0.9448    0.9352    0.9293    0.9287    0.9283    0.9287    0.9280    0.9299    0.9299    0.9278
0.9296    0.9284    0.9306    0.9302    0.9311    0.9283    0.9290    0.9302    0.9281    0.9299
0.9283    0.9318];

TFUplot6 = [0.9909    0.9858    0.9850    0.9837    0.9825    0.9813    0.9796    0.9782
0.9783    0.9784    0.9787    0.9782    0.9762    0.9694    0.9615    0.9513    0.9399    0.9273
0.9115    0.8966    0.8873    0.8864    0.8857    0.8863    0.8853    0.8883    0.8883    0.8849
```

```
 0.8878     0.8859    0.8893    0.8887    0.8902    0.8857    0.8869    0.8887    0.8854    0.8882
 0.8857     0.8914];
TFUplot7 = [0.9925     0.9882    0.9875    0.9864    0.9854    0.9844    0.9829    0.9817
 0.9818     0.9818    0.9821    0.9817    0.9801    0.9750    0.9690    0.9612    0.9526    0.9430
 0.9310     0.9197    0.9127    0.9120    0.9114    0.9119    0.9112    0.9134    0.9134    0.9108
 0.9131     0.9116    0.9142    0.9137    0.9150    0.9115    0.9124    0.9137    0.9112    0.9133
 0.9114     0.9158];
TFUplot8 = [0.9938     0.9900    0.9894    0.9884    0.9876    0.9866    0.9853    0.9843
 0.9844     0.9844    0.9846    0.9843    0.9831    0.9792    0.9745    0.9686    0.9621    0.9548
 0.9456     0.9370    0.9316    0.9311    0.9307    0.9309    0.9305    0.9321    0.9321    0.9301
 0.9320     0.9308    0.9327    0.9323    0.9334    0.9308    0.9314    0.9324    0.9305    0.9321
 0.9306     0.9341];
TFUplot9 = [0.9947     0.9914    0.9908    0.9900    0.9892    0.9884    0.9872    0.9863
 0.9864     0.9864    0.9866    0.9863    0.9854    0.9824    0.9789    0.9744    0.9694    0.9639
 0.9569     0.9504    0.9462    0.9459    0.9455    0.9457    0.9455    0.9467    0.9466    0.9451
 0.9466     0.9457    0.9471    0.9468    0.9477    0.9457    0.9461    0.9469    0.9454    0.9466
 0.9454     0.9483];
TFUplot10 = [0.9955     0.9925    0.9920    0.9912    0.9905    0.9898    0.9887    0.9879
 0.9880     0.9880    0.9881    0.9879    0.9872    0.9850    0.9823    0.9790    0.9753    0.9712
 0.9659     0.9611    0.9579    0.9577    0.9574    0.9575    0.9574    0.9583    0.9582    0.9570
 0.9582     0.9575    0.9586    0.9583    0.9591    0.9576    0.9579    0.9584    0.9573    0.9582
 0.9573     0.9595];

plot11 = [0.9870    0.9805    0.9794    0.9777    0.9762    0.9747    0.9726    0.9707    0.9709
 0.9710     0.9710    0.9623    0.9538    0.9436    0.9314    0.9165    0.9001    0.8820    0.8597
 0.8386     0.8255    0.8241    0.8232    0.8240    0.8226    0.8268    0.8268    0.8221    0.8261
 0.8234     0.8283    0.8275    0.8295    0.8231    0.8248    0.8274    0.8227    0.8268    0.8233
 0.8310];
plot12 = [0.9879    0.9816    0.9805    0.9789    0.9775    0.9760    0.9739    0.9721    0.9723
 0.9723     0.9728    0.9703    0.9623    0.9527    0.9412    0.9270    0.9111    0.8937    0.8720
 0.8514     0.8387    0.8373    0.8364    0.8373    0.8359    0.8399    0.8400    0.8354    0.8393
 0.8366     0.8414    0.8406    0.8425    0.8364    0.8380    0.8405    0.8360    0.8399    0.8365
 0.8441];
plot13 = [0.9892    0.9833    0.9823    0.9809    0.9795    0.9781    0.9761    0.9744    0.9746
 0.9746     0.9750    0.9744    0.9747    0.9705    0.9605    0.9475    0.9328    0.9165    0.8960
 0.8766     0.8646    0.8633    0.8625    0.8633    0.8619    0.8658    0.8658    0.8615    0.8652
 0.8627     0.8672    0.8664    0.8683    0.8624    0.8639    0.8663    0.8620    0.8657    0.8625
 0.8697];
plot14 = [0.9898    0.9842    0.9832    0.9818    0.9805    0.9792    0.9772    0.9756    0.9757
 0.9758     0.9762    0.9756    0.9758    0.9755    0.9700    0.9577    0.9436    0.9279    0.9080
 0.8892     0.8776    0.8763    0.8755    0.8763    0.8750    0.8787    0.8788    0.8745    0.8781
 0.8757     0.8800    0.8793    0.8811    0.8755    0.8769    0.8792    0.8751    0.8787    0.8756
 0.8825];

normalize=Total_fuel_used_GT_only(1);
figure
hold on;
ylim([0.8 1])
%plot(1:FC_available,Total_fuel_saved/normalize)
plot(1:FC_available,Total_fuel_used_hybrid/normalize)
plot(1:FC_available,Total_fuel_used_GT_only/normalize)
%plot(1:FC_available,plot11)
%plot(1:FC_available,plot12)
%plot(1:FC_available,plot13)
%plot(1:FC_available,plot14)
%plot(1:FC_available,TFUplot10)
ylabel('Total Fuel Consumption (ratioed to GT only plant)')
xlabel('Number of Installed Fuel Cells')
```